

# 1 The effects of mixing on Age of Air

H. Garny,<sup>1</sup> T. Birner,<sup>2</sup> H. Bönisch,<sup>3</sup> F. Bunzel<sup>4</sup>

---

Corresponding author: H. Garny, Deutsches Zentrum für Luft- und Raumfahrt, Institut für Physik der Atmosphäre, Oberpfaffenhofen, Germany (hella.garny@dlr.de)

<sup>1</sup>Deutsches Zentrum für Luft- und Raumfahrt, Institut für Physik der Atmosphäre, Oberpfaffenhofen, Germany.

<sup>2</sup>Department of Atmospheric Science, Colorado State University, Fort Collins, CO, USA.

<sup>3</sup>Institute for Atmospheric and Environmental Sciences, Goethe University Frankfurt, Frankfurt am Main, Germany.

<sup>4</sup>Max Planck Institute for Meteorology, Hamburg, Germany.

**Abstract.** Mean age of air (AoA) measures the mean transit time of air parcels along the Brewer-Dobson circulation (BDC) starting from their entry into the stratosphere. AoA is determined both by transport along the residual circulation and by two-way mass exchange (mixing). The relative roles of residual circulation transport and two-way mixing for AoA, and for projected AoA changes are not well understood. Here, effects of mixing on AoA are quantified by contrasting AoA with the transit time of hypothetical transport solely by the residual circulation. Based on climate model simulations, we find additional aging by mixing throughout most of the lower stratosphere, except in the extratropical lowermost stratosphere where mixing reduces AoA. We use a simple Lagrangian model to reconstruct the distribution of AoA in the GCM, and to illustrate the effects of mixing at different locations in the stratosphere. Predicted future reduction in AoA associated with an intensified BDC is equally due to faster transport along the residual circulation as well as reduced aging by mixing. A tropical leaky pipe model is used to derive a mixing efficiency, measured by the ratio of the two-way mixing mass flux and the net (residual) mass flux across the subtropical boundary. The mixing efficiency remains close to constant in a future climate, suggesting that the strength of two-way mixing is tightly coupled to the strength of the residual circulation in the lower stratosphere. This implies that mixing generally amplifies changes in AoA due to uniform changes in the residual circulation.

## 1. Introduction

24 A clear conceptual picture of the stratospheric transport circulation, the Brewer-Dobson  
25 circulation (BDC), has evolved over the last decades [reviewed in e.g. *Butchart, 2014*;  
26 *Plumb, 2002*; *Shepherd, 2007*]. The zonal mean part of this transport circulation can be  
27 characterized by mean mass flux as given by the residual mean meridional circulation  
28 (residual circulation hereafter; see Sec. 2.2), and by two-way exchange of air masses. The  
29 residual circulation consists of upwelling in the tropics, poleward transport and down-  
30 welling in mid-to high latitudes, as illustrated in Fig. 1 (black arrows). Strong two-way  
31 mass exchange is caused by breaking planetary waves, leading to strong quasi-horizontal  
32 stirring, displacing air masses over thousands of kilometers [*McIntyre and Palmer, 1984*].  
33 Turbulent mixing toward smaller scales and eventually molecular diffusion results in the  
34 irreversibility of the displacement of air. The two-way mass exchange resulting from the  
35 entire cascade from stirring by planetary waves to turbulent mixing is referred to as ”(two-  
36 way) mixing“ in the context of this work [see also *Shuckburgh and Haynes, 2003*; *Plumb,*  
37 *2002*]. Enhanced wave breaking leads to strong two-way mixing in the extratropical surf  
38 zone [*McIntyre and Palmer, 1984*], illustrated by blue arrows in Fig. 1. While the tropics  
39 are generally well isolated from the extratropics by the subtropical barrier [e.g. *Trepte*  
40 *and Hitchman, 1992*], two-way mixing across this barrier can occur, for example due to  
41 breaking planetary waves [e.g. *Randel et al., 1993*, red arrows in Fig. 1].

42 Stratospheric age of air is defined as the transit time of an air parcel since its entry into  
43 the stratosphere [*Hall and Plumb, 1994*]. Thus, age of air is a measure of the integrated  
44 effect of all transport processes that affect the pathway of an air parcel through the

45 stratosphere. Mean age of air (AoA) is the first moment of the transit time distribution  
46 at a certain location in the stratosphere, and is often used to quantify the strength of  
47 the transport circulation in the stratosphere (the BDC). It has been long recognized from  
48 conceptual model studies that mixing between the tropics and extratropics can increase  
49 AoA globally [*Neu and Plumb, 1999*]. The additional aging is caused by the "recirculation"  
50 of air parcels through the stratosphere, as illustrated in Fig. 1: An air parcel enters the  
51 stratosphere (A) and travels along the residual circulation to the extratropics (B). From  
52 there, it can be mixed back into the tropics (B to C), and thus re-circulates along the  
53 residual circulation (C to D). The parcel's age increases steadily while performing multiple  
54 circuits through the stratosphere. Thus, the process of *mixing* (transition B to C) affects  
55 the air parcel's age as it leads to *recirculation* (C to D). Note that due to the definition  
56 of mixing as two-way mass exchange, another air parcel of same mass had to be mixed  
57 from C to B at the same time. In the following, we refer to the effect of mixing on AoA  
58 as *aging by mixing*.

59 AoA can be estimated from observations of quasi-passive tracers with monotonically  
60 increasing concentrations, such as  $SF_6$  [*Bönisch et al., 2009*]. *Strahan et al.* [2009] used  
61 ascent rates from the observed tropical water vapor tape recorder to estimate tropical  
62 modal AoA (i.e. the most probable transit time). The difference of modal AoA to mean  
63 AoA was then used to empirically quantify the effects of mixing on AoA. However, it is  
64 important to note that it is impossible to directly measure the residual circulation, so that  
65 only the integrated effect of all transport processes can be estimated from observations.  
66 Therefore, the relationship between the residual circulation and AoA needs to be better  
67 understood.

68 In the light of recent results on trends in the strength of the BDC, the understanding  
69 of mechanisms that drive changes in the circulation came into focus. While global models  
70 project a strengthened residual circulation in a changing climate, and simultaneously a  
71 decrease in AoA [*Butchart et al.*, 2010], evidence of trends in AoA from observational  
72 estimates is weak [*Engel et al.*, 2009; *Stiller et al.*, 2012; *Diallo et al.*, 2012; *Bönisch et al.*,  
73 2011]. In models, so far the focus of studies was on the mechanisms for the intensification  
74 of the residual circulation [*Garcia and Randel*, 2008; *McLandress and Shepherd*, 2009;  
75 *Calvo and Garcia*, 2009; *Shepherd and McLandress*, 2011; *Okamoto et al.*, 2011; *Bunzel*  
76 *and Schmidt*, 2013; *Oberländer et al.*, 2013]. *Austin and Li* [2006] found that empirically,  
77 AoA is linearly linked to tropical upwelling. *Li et al.* [2012] investigated changes in age  
78 spectra, and found that both the modal AoA and the tail of the spectrum contribute to  
79 the decrease of mean AoA, concluding that mixing plays a substantial role for the decrease  
80 in AoA. However, the relationship between the residual circulation and AoA, and possible  
81 impacts of changes in two-way mixing on AoA are not well understood. *Ray et al.* [2010]  
82 emphasize that trends in AoA are strongly sensitive to possible changes in two-way mixing  
83 between the tropics and extratropics.

84 In this paper, we seek to gain better understanding of the effects of mixing on AoA. To  
85 this end, we use simulations with a general circulation model (GCM) that provides AoA  
86 together with consistent information on the residual circulation. The residual circulation  
87 transit time (RCTT) – the transit time of hypothetical transport solely by the residual  
88 circulation, is obtained as described in Sec. 2 and used in Sec. 3 to quantify the effect  
89 of mixing on AoA. To better understand those effects, two conceptual model approaches  
90 are used: the tropical leaky pipe (TLP) model (Sec. 4.1), which assumes two columns of

well-mixed air (a tropical and an extratropical column), is used to quantify the strength of mixing across the subtropical barrier that is necessary to explain the aging by mixing in the GCM. In addition, a simple Lagrangian random walk model (Sec. 4.2) is used to reconstruct the latitudinal distribution of aging by mixing and to illustrate the effects of mixing at different locations in the stratosphere. To elucidate the role of mixing for long-term changes in AoA and possible coupling of the mixing strength and the residual circulation, three equilibrium climate states are compared in Sec. 5.

## 2. Methods

### 2.1. Model description

The comprehensive GCM used in this study is ECHAM6 [Stevens *et al.*, 2013]. Simulations were performed in the time-slice mode, i.e. under stationary boundary conditions, for preindustrial (1860), present-day (1990), and future (2050) climate states. These simulations are referred to as TS1860, TS1990 and TS2050 in the following. For each time slice 50 years were simulated after a spin-up period of 5 years. Prescribed boundary conditions including greenhouse gas (GHG) concentrations (including also chlorofluorocarbons), sea surface temperatures (SST), sea ice coverage (SIC), ozone distribution, and aerosols were applied to simulate the different climate states. Both SST and SIC input data were taken from the output of coupled atmosphere-ocean GCM simulations performed with ECHAM5 [Röckner *et al.*, 2003] coupled to MPIOM [Max Planck Institute Ocean Model; Marsland, 2003], which were carried out for CMIP3. For the future time slice boundary conditions follow the RCP4.5 scenario [Vuuren *et al.*, 2011], except SST and SIC that are taken from a simulations that followed the SRES A1B scenario [Nakicenovic and Swart, 2000]. The CMIP5 simulations, that follow the RCP4.5 scenario, were not completed by the start

112 of the experiments used in this study. However, the inconsistency between the SST/SIC  
 113 dataset and the prescribed atmospheric conditions is small as both the SRES A1B and  
 114 the RCP4.5 scenarios assume steadily rising CO<sub>2</sub> concentrations to levels around 500 ppm  
 115 in 2050 [Vuuren *et al.*, 2011]. In all simulations the horizontal resolution is T63 (1.9° x  
 116 1.9°), while the vertical model domain extends up to 0.01 hPa with 47 levels. For details  
 117 see *Bunzel and Schmidt* [2013].

## 2.2. Calculation of residual circulation transit time and age of air

118 Residual circulation transit times (RCTTs) are calculated following *Birner and Bönisch*  
 119 [2011]. The principle is based on calculating backward trajectories that are driven by the  
 120 residual mean meridional and vertical winds. The residual velocities ( $\bar{v}^*$ ,  $\bar{w}^*$ ) are calcu-  
 121 lated from 6-hourly model output of meridional and vertical winds ( $v, w$ ) and potential  
 122 temperature ( $\Theta$ ) as follows [Equ. 3.5.1 in *Andrews et al.*, 1987]:

$$\bar{v}^* = \bar{v} - \frac{1}{\rho_0} \frac{\partial}{\partial z} (\rho_0 \overline{v' \Theta'} / \frac{\partial \Theta_0}{\partial z}) \quad (1)$$

$$\bar{w}^* = \bar{w} + \frac{1}{r \cos \phi} \frac{\partial}{\partial \phi} (\overline{v' \Theta'} / \frac{\partial \Theta_0}{\partial z}) \quad (2)$$

123 Monthly mean velocities are then used to calculate the backward trajectories in the  
 124 latitude-height plane with a standard fourth-order Runge-Kutta integration. The back-  
 125 ward trajectories are initialized on a grid with 35 latitudes (spaced every 5°) and on  
 126 10 pressure levels (200, 170, 150, 120, 100, 70, 50, 30, 20 and 10 hPa). The backward  
 127 trajectories are terminated when they reach the thermal tropopause (calculated follow-  
 128 ing the WMO definition), and the elapsed time is the residual circulation transit time.  
 129 Trajectories are initialized in the middle of a month, and are calculated backward using  
 130 the varying residual velocities and tropopause values. RCTTs are calculated for every

131 month of the last 10 years of each time-slice simulation. In the following, annual mean  
132 climatological values of RCTTs are used (i.e. averaged over 120 values per grid point).  
133 As the inter-annual variability in annual mean AoA is less than 10% everywhere, 10 years  
134 of data are sufficient to represent the mean state of the simulations. We focus here on  
135 annual mean values as we are mainly interested in mean effects of mixing on long-term  
136 changes. For a discussion of the seasonal cycle in RCTT see *Birner and Bönisch* [2011].

137 In GCM simulations with ECHAM6 a passive tracer is used to derive AoA. Following  
138 *Hall and Plumb* [1994] this tracer is initialized in the lowermost model level between  
139 5°S and 5°N with concentrations increasing linearly over time. The time lag in tracer  
140 concentrations between a certain grid point in the stratosphere and the tropical tropopause  
141 provides an estimation of AoA at this stratospheric grid point. The reference point at  
142 the tropical tropopause for age tracer concentrations is set between 10°S and 10°N as the  
143 height of the thermal tropopause (i.e. consistent with the RCTT calculations).

### 3. Effects of Mixing on Age of Air in a GCM

144 AoA averaged over 10 years from the TS1990 simulation is shown in Fig. 2. In addi-  
145 tion, the hypothetical age if air was transported only by the residual circulation (RCTT)  
146 calculated over the same time period than AoA is shown. The RCTT considerably differs  
147 from AoA both in magnitude and structure. While AoA isolines are orientated quasi-  
148 horizontally, RCTT has a strong meridional gradient in particular in middle to high  
149 latitudes. In contrast to the distribution of AoA, RCTT clearly follows the structure of  
150 the residual mean circulation (white contours in Fig. 2). The strong gradient in RCTT  
151 from mid- to high latitudes marks the different residual circulation branches, as discussed  
152 by *Birner and Bönisch* [2011]: The shallow branch consists of upward net mass transport

153 in the (sub-)tropics, poleward and downward in mid-latitudes, with air mostly remain-  
154 ing below about 70 hPa. The deep branch, on the other hand, consists of upward net  
155 mass transport in the deep tropics and downward at high latitudes. The branches are  
156 also manifested in distinct regions of wave breaking: the shallow branch is predominantly  
157 driven by wave breaking in the subtropical lower stratosphere, while the deep branch is  
158 predominantly driven by wave breaking in the vicinity of the polar night jet in the middle  
159 stratosphere.

160 The advantage of global model data is the availability of AoA and consistent with  
161 it the residual circulation, and thus RCTT, so that AoA can be compared with those  
162 hypothetical transit times. The difference between AoA and RCTT can be interpreted  
163 as the modification of the transit time following net air mass transport by additional  
164 processes, including quasi-horizontal two-way mixing, but also vertical diffusion or any  
165 (numerical) uncertainties in the calculation of AoA and RCTT. The representation of  
166 advection in the model certainly affects the strength of the simulated two-way mixing  
167 mass flux, so that numerical diffusion is implicitly included in our definition of two-way  
168 mixing (this is further discussed in Sec. 6). We assume in the following that other  
169 numerical uncertainties (e.g. in the calculation of RCTT) are small, and thus that the  
170 difference between AoA and RCTT is caused in by two-way mixing. We refer to the  
171 difference between AoA and RCTT as *aging by mixing*.

172 In most of the stratosphere, air is older than if it was only transported along the residual  
173 circulation (see lower panel of Fig. 2). Aging by mixing maximizes in mid-latitudes and  
174 increases with height. In the lowermost extratropical stratosphere and close to the poles,  
175 mixing reduces transit times – here, air is younger than for purely residual transport.

176 The distribution of aging by mixing does not necessarily resemble the distribution of  
177 mixing strength, measured for example by effective diffusivity [*Haynes and Shuckburgh,*  
178 2000]. Neither does aging by mixing maximize in regions of wave breaking. As will be  
179 shown in Sec. 4, aging by mixing at one particular point in the stratosphere can be  
180 induced by mixing remote to this point. Furthermore, mixing in different regions of the  
181 atmosphere has varying impacts on AoA. Therefore, it cannot be expected that the effect  
182 of mixing on AoA (i.e. aging by mixing) is locally related to the mixing strength.

## 4. Effects of Mixing on Age of Air in Conceptual Models

### 4.1. The Tropical Leaky Pipe Model

#### 183 4.1.1. Formulation of the Tropical Leaky Pipe Model

The tropical leaky pipe (TLP) model, described in *Neu and Plumb* [1999] (NP99 in the following), divides the stratosphere into the tropical pipe and the well-mixed surf zones of the SH and NH. It is assumed that (1) mixing within the surf zones is fast compared to mixing across the boundary and (2) the surf zone extends all the way to the pole (i.e. the polar regions with their seasonal barrier are neglected). Thus, the model is essentially 1-dimensional (vertical coordinate) with 3 columns that can interact. The tropical pipe corresponds to the upwelling region (see Fig. 1), and the surf zones to the downwelling region. Vertical motion within each region is prescribed. Furthermore, horizontal exchange between the tropics and the surf zones is allowed. We further make the following simplifications to the model: First, vertical diffusion is neglected. In NP99 it was shown that AoA using the vertical diffusivity as reported by *Sparling et al.* [1997] is very similar to AoA in the nondiffusive case, except close to the extratropical tropopause. Second, we assume that the hemispheres are symmetric (i.e. the properties of the northern surf zone

equal those of the southern surf zone). With these simplifications, the formulation of the tracer budget equations for a passive tracer with mixing ratio  $\sigma$  in the tropics (T) and surf-zones (SZ) with sources  $S_T$  and  $S_{SZ}$  are given by:

$$\frac{\partial \sigma_T}{\partial t} - S_T = -w_T \frac{\partial \sigma_T}{\partial z} - \frac{1}{\alpha} \epsilon \lambda (\sigma_T - \sigma_{SZ}) \quad (3)$$

$$\frac{\partial \sigma_{SZ}}{\partial t} - S_{SZ} = -w_{SZ} \frac{\partial \sigma_{SZ}}{\partial z} + (\epsilon + 1) \lambda (\sigma_T - \sigma_{SZ}) \quad (4)$$

where  $w_T$  and  $w_{SZ}$  are the vertical velocities in the tropics and surf-zones, respectively, and  $\alpha$  is defined as the ratio of tropical to the extratropical mass ( $\alpha = M_T / (2M_{SZ})$ , where  $M_{SZ}$  is the mass in either hemisphere, as they are assumed to be symmetric). The horizontal transport between tropics and extratropics is described by two relaxation factors  $\lambda$  and  $\epsilon$ . The factor  $\lambda$  is defined as the horizontal transport that is determined by mass continuity by the prescribed vertical velocities (i.e.  $\partial_y \bar{v}^* = -1/\rho \partial_z (\rho \bar{w}^*)$ ). Following NP99,  $\lambda$  is calculated as

$$\lambda = -\frac{1}{M_T} \frac{\partial (M_T w_T)}{\partial z} \quad (5)$$

184 The factor  $\epsilon$ , on the other hand, describes the two-way mass exchange (i.e. what we  
185 describe as “mixing”) and can be chosen freely.  $\epsilon$  is defined as the ratio of the mass flow  
186 from the surf zones to the tropics to the net mass flux between tropics and the surf zones.  
187 The net mass flux is the horizontal motion that is determined by mass continuity via the  
188 prescribed vertical motion (given by  $\lambda$ ), and corresponds to transport by  $\bar{v}^*$ . If  $\epsilon = 0$ ,  
189 there is no mixing, and if  $\epsilon = 2$ , the mass flow due to mixing in either direction is twice  
190 as large as the net mass flow. We will refer to  $\epsilon$  in the following as *mixing efficiency*.

191 If it is further assumed that  $w_T$  and  $\epsilon$  are constant with height, a simple analytical  
192 solution for the tropical age ( $\Gamma_T$ ) and age in the surf zones ( $\Gamma_{SZ}$ ) in the TLP model can

193 be formulated (for the derivation see Sec. 3 in NP99):

$$\Gamma_T = \frac{\alpha + \epsilon(\alpha + 1)}{\alpha w_T} (z - z_T) \quad (6)$$

$$\Gamma_{SZ} = \frac{\alpha + \epsilon(\alpha + 1)}{\alpha w_T} (z - z_T) + \frac{(1 + \alpha)}{\lambda} \quad (7)$$

194 The vertical coordinate  $z$  is the equivalent height above the extratropical tropopause  
 195 ( $z = 0$ ), and  $z$  is parallel to age isopleth (see NP99).  $z_T$  is the height of the tropical  
 196 tropopause.

#### 197 4.1.2. Aging by Mixing in the Tropical Leaky Pipe Model

The diagnostics AoA and RCTT can be described with the TLP model such that AoA  
 is the full age with mixing efficiency  $\epsilon$  ( $\Gamma^\epsilon$ ), while RCTT is the solution with  $\epsilon = 0$  ( $\Gamma^0$ ).  
 From Equ. 6 it follows that aging by mixing in the tropics ( $A_{mix}^T$ ) equals

$$A_{mix}^T = \Gamma_T^\epsilon - \Gamma_T^0 = \epsilon \left(1 + \frac{1}{\alpha}\right) \frac{z - z_T}{w_T} \quad (8)$$

198 Aging by mixing in the surf zones calculated as  $\Gamma_{SZ}^\epsilon - \Gamma_{SZ}^0$  equals aging by mixing in the  
 199 tropics, i.e. a certain mixing efficiency causes air to age as much in the tropics as in the  
 200 extratropics.  $A_{mix}$  is always positive above the tropical tropopause and negative below,  
 201 in agreement with the result from the GCM that mixing leads to an increase of AoA in  
 202 most of the stratosphere and a decrease in the extratropical lowermost stratosphere.

203 According to the TLP formulation, aging by mixing is not only a function of the mixing  
 204 efficiency, but also of the vertical velocity – or in other words, the residual circulation  
 205 strength.  $A_{mix}$  is proportional to  $\epsilon$  (i.e. the higher the mixing efficiency, the larger aging  
 206 by mixing) but indirectly proportional to  $w_T$  (i.e. the larger the vertical velocity, the  
 207 smaller the additional aging due to mixing). The increase of aging by mixing with the  
 208 mixing efficiency was explained in NP99 by the "re-circulation" effect, as was described

209 in the Introduction: Mixing between young tropical air and older air in the surf zones  
210 adds older air into the tropics. This older air re-circulates upward in the tropical pipe and  
211 eventually back into the surf zone, thus eventually conducting multiple circuits through  
212 the stratosphere. Thereby older air is added both in the tropics and surf zones, aging the  
213 air in both regions by the same amount. The re-circulation will be examined further with  
214 a Lagrangian random walk model in Sec. 4.2.

215 While a higher mixing efficiency causes more air parcels to re-circulate, thereby in-  
216 creasing aging by mixing, the velocity  $w_T$  controls the speed of the re-circulation. If  $w_T$   
217 increases, the additional circuits air parcels travel take less time, and aging by mixing  
218 decreases. Thus, even under a constant mixing efficiency, aging by mixing can change  
219 if the speed of the residual circulation changes. In principle, an increase in the vertical  
220 velocity  $w_T$  could be counteracted by changes in the mixing efficiency  $\epsilon$  in a way that AoA  
221 remains unaffected. However, as will be discussed in Sec. 5, mixing by wave breaking is  
222 not independent of residual transport.

### 223 **4.1.3. Mixing efficiency in the GCM derived with the Tropical Leaky Pipe** 224 **Model**

225 The TLP model in the formulation as described above has two free parameters that  
226 can be chosen: the tropical vertical velocity  $w_T$  and the mixing efficiency  $\epsilon$ . The vertical  
227 velocity can be diagnosed easily from the GCM data as the mean  $\bar{w}^*$  in the tropics.  
228 We choose a latitude band of 30°S-30°N as tropical pipe, as these latitudes capture the  
229 approximate region of upwelling best (the turnaround latitudes lie between 25-40°N/S,  
230 depending on height).

The analytical solution of the TLP model with a height dependent vertical velocity  $w_T(z)$  (see Equ. 9-10 of NP99) for tropical AoA is:

$$\Gamma_T(z) = \int_{z_T}^z \frac{1}{w_T(z')} dz' + \epsilon \frac{(\alpha + 1)}{\alpha} \left( \int_{z_T}^z \frac{1}{w_T(z')} dz' + H \left( \frac{1}{w_T(z)} - \frac{1}{w_T(z_T)} \right) \right) \quad (9)$$

231 where  $H$  is the scale height (7 km). In the following we will approximate the mean tropical  
 232 profiles of AoA and RCTT using this solution of the TLP model. RCTT can be calculated  
 233 from the TLP model using tropical vertical velocities from the GCM as input and setting  
 234  $\epsilon$  to zero. As shown in Fig. 3 the tropical RCTT from the GCM (solid blue line) are  
 235 reasonably well reproduced with the TLP Model (dashed blue line). Deviations are  $\leq$   
 236 10% above 50 hPa and  $\leq$  33% below; the high relative deviation at the lowest level is due  
 237 to the small absolute value of transit time here.

238 For given vertical velocities, the difference between AoA and RCTT depends only on  
 239 the mixing efficiency  $\epsilon$ . Thus,  $\epsilon$  can be derived from the tropical AoA and RCTT profiles  
 240 as the best fit of the TLP model to the GCM profiles. The best fit over all layers in the  
 241 lower stratosphere (tropopause to 10 hPa) is obtained with a mixing efficiency of  $\epsilon = 0.32$   
 242 for the TS1990 simulation. Thus, given the definition of  $\epsilon$  in Sec. 4.1.1, the mixing mass  
 243 flux across the subtropical barrier is about a third as strong as the net mass flux into the  
 244 extratropics. The result for  $\epsilon$  is robust (within 10%) for latitude bands within the range  
 245 of the border of the tropical pipe (i.e. between 25-40°N/S). The fit with the TLP model  
 246 reproduces tropical AoA from the GCM reasonably well, mostly with deviations  $\leq$  10%  
 247 expect around 70 hPa, where deviations are larger (30%). Fitting the TLP model only at  
 248 levels above 70 hPa does, however, result in only slight changes of the mixing efficiency  
 249 (0.33 instead of 0.32) and further results are not affected. The larger deviations in the  
 250 lower levels might be caused either by the simplified assumption of a constant width of the

251 tropical pipe with height (close to the tropopause, the tropical pipe narrows), or might  
252 indicate that mixing efficiencies in the shallow branch differ from those in the deep branch  
253 of the BDC. For the lower levels, a smaller mixing efficiency of about 0.2 results in a better  
254 fit to AoA.

255 As discussed above, AoA increases with the mixing efficiency, as shown by the dashed  
256 lines in Fig. 3. These cases would represent a stronger or weaker relative mixing mass flux  
257 compared to the net mass flux. How the net and mixing mass flux are related is further  
258 discussed in Sec. 5.

## 4.2. A Lagrangian random walk model of mixing effects

259 The TLP model used in the last section is suitable to quantify effects of mixing across  
260 the subtropical barrier on the tropical and extratropical mean AoA profiles. However,  
261 the latitudinal structure of aging by mixing found in the GCM cannot be captured by  
262 the TLP model due to its setup. To examine the causes for the distribution of aging  
263 by mixing, and to analyze the role of mixing at different locations in the stratosphere,  
264 we developed a simple Lagrangian transport model (Sec. 4.2.2 and Appendix A). We  
265 start by illustrating effects of mixing on AoA in the Lagrangian framework using simple  
266 conceptual experiments.

### 4.2.1. Conceptual experiments on recirculation and mixing effects

268 The TLP model predicts that tropical-extratropical mixing of a certain strength in-  
269 creases AoA as much in the tropics as in the extratropics through the effect of re-circulation  
270 of air parcels (Equ. 6; also discussed in NP99). This effect can be illustrated with the  
271 following simple Lagrangian experiment:

272 We use a trajectory calculated from residual velocities (see Fig. 4a). Along the tra-  
273 jectories, points that are equally spaced in time (with  $\Delta t=5$  days) are defined, and each  
274 point is assigned with 100 air parcels of equal mass. Air parcels are advected along the  
275 trajectories, and their transit time increases as they do so. Two-way mixing is included in  
276 the model by instantaneously exchanging a given fraction of randomly chosen air parcels  
277 between pre-defined mixing points. As mixing is likely to take place along isentropic sur-  
278 faces in the real atmosphere, we use the intersections of the trajectories with isentropic  
279 surfaces as mixing points. For this first simple experiment we chose the 380 K level and  
280 exchange an arbitrarily chosen fraction of  $\mu = 10\%$  of randomly selected parcels between  
281 the tropical and the extratropical mixing point. The random exchange of air parcels  
282 essentially results in a random walk of the air parcels.

283 When running the model for a sufficient amount of time, a new equilibrium AoA is  
284 reached that is greater than AoA without mixing at all locations between the two mixing  
285 points (compare red and black lines in Fig. 4c), as was predicted by the TLP model. It  
286 can be clearly seen from the age spectrum at  $50^\circ\text{N}$  that the additional aging is caused by  
287 in-mixing of old air from the extratropics to the tropics, which subsequently recirculates  
288 along the deep branch. Below the extratropical mixing point, AoA is unchanged when  
289 mixing is included. This simple experiment illustrates that this is due to a cancellation of  
290 old re-circulating air and young air that was mixed in from the tropical lower stratosphere:  
291 the age spectrum at  $85^\circ\text{N}$  (Fig. 4c) shows that as much very young (less than 1 year) air  
292 parcels are found as old air parcels, that were mixed to the tropics, recirculate along the  
293 trajectory and eventually reach the region below the extratropical mixing point. They

294 have aged exactly the age difference between the tropical and extratropical mixing point,  
295 and thus exactly compensate for the younger tropical air.

296 Thus, mixing between the tropics and extratropics at a certain level only affects air  
297 above this level, and the additional aging depends only on the age difference between the  
298 tropics and extratropics. It follows that mixing at lower levels will have an overall larger  
299 impact on AoA than mixing at higher levels. Note that this is consistent with the TLP  
300 model, that predicts that mixing leads to aging of air that is equally strong in the tropics  
301 as in the extratropics (see Equ. 6). As mixing at a certain level affects tropical AoA  
302 only above this level, it follows that also extratropical AoA must be unaffected by mixing  
303 below the level of mixing.

304 In the TLP model, the effects of mixing across the subtropical barrier are examined,  
305 while mixing within the extratropics is assumed to be very strong. This is a valid as-  
306 sumption as long as the strength of mixing within the extratropics does not affect the  
307 extratropical mean AoA profile (and thus not tropical mean AoA, according to the ar-  
308 guments above). In the following, we illustrate with the simple Lagrangian model that  
309 mixing within the extratropics can have an effect on extratropical mean AoA given that  
310 air parcels take different pathways, for example along the different branches of the BDC.  
311 However, this effect is small compared to mixing across the subtropical barrier. We include  
312 a second trajectory that represents the shallow branch of the circulation and terminates  
313 at the tropopause at 60°N (Fig. 4b). A fraction of  $\mu = 10\%$  of the air parcels are mixed  
314 between the extratropical intersects of the 380 K isentropic level and the two trajectories,  
315 i.e. between about 55°N to 80°N. Mixing within the extratropics adds younger air to the  
316 lower part of the deep branch trajectory, and older air to the shallow branch trajectory

(Fig. 4d), thereby flattening the age gradient in the extratropics. Thus, mixing within the  
extratropics has a strong local effect. The mean extratropical AoA profile can be affected  
by mixing in case the remaining time of the mixed air parcels in the stratosphere differs.  
Such a difference in the remaining time can occur essentially depending on the shape of  
the circulation and the slope of the tropopause. For the example of mixing at 380 K, a  
small decrease in AoA averaged over all air parcels is found to be induced by mixing.  
Depending on the altitude of mixing, the net effect on AoA can be positive or negative,  
but is never larger than a few percent in the current example. For comparison, mixing  
of the same strength between tropics and extratropics has a net effect on AoA of almost  
50%. As the difference of the remaining time in the stratosphere is much smaller for air  
parcels located in the extratropics compared to parcels mixed between tropics and extra-  
tropics this is expected. However, as mixing in the extratropics has a strong local effect,  
we will investigate in the following how the distribution of aging by mixing is influenced  
by mixing at different locations.

#### 4.2.2. Distribution of aging by mixing

We extend the Lagrangian model to a set of 20 trajectories that terminate between  $40^\circ$   
and  $85^\circ\text{N}$  at the tropopause. This set of 20 trajectories represents mean transport along  
different branches of the residual circulation in the Northern Hemisphere. The transit  
times along the trajectories are shown in Fig. 5a.

Mixing points are defined as the intersects of trajectories with 20 isentropic levels be-  
tween 340 K and 2000 K. The calculation of mixing between all the intersects on one  
isentropes would become quickly excessive when adding more trajectories ( $0.5 \cdot M(M-1)$  in-  
terchanges for  $M$  intersects). Thus, air parcels are grouped into tropical and extratropical

340 parcels, and mixing is performed within and between those groups. Thus, three mixing  
341 events are possible at each isentropic level: 1) mixing within the tropics, 2) mixing of  
342 tropical and extratropical air and 3) mixing within the extratropics. For each class of  
343 mixing operation, a height dependent mixing strength ( $\mu_{Tr}$ ,  $\mu_{TrEx}$  and  $\mu_{Ex}$ , respectively)  
344 is prescribed as follows: mixing within the tropics and within the extratropics is set to  
345  $\mu_{Ex} = \mu_{Tr} = 0.25$ . The model is not sensitive to the choice of  $\mu_{Tr}$ . Mean profiles are also  
346 not sensitive to  $\mu_{Ex}$ , and it is set to best resemble the latitudinal distribution of AoA. The  
347 critical parameter is the mixing strength between tropics and extratropics,  $\mu_{TrEx}$ . We set  
348 the tropical-extratropical mixing parameter by assuming that the two-way mixing mass  
349 flux is proportional to the net mass flux, which is a realistic assumption as will be shown  
350 in Sec. 5. The ratio of two-way mass flux to net mass flux is set to the mixing efficiency  
351 as calculated with the TLP model fit (Sec. 4.1). Details on the settings of the Lagrangian  
352 model and sensitivities to those settings can be found in Appendix A.

353 AoA after an integration over  $10 \cdot N$  time steps (where  $N$  is the number of time steps it  
354 takes an air parcels to travel along the longest trajectory) is shown in Fig. 5b. Mixing leads  
355 to additional aging of air in most of the stratosphere, only in the high latitude lowermost  
356 stratosphere age decreases due to mixing. The profiles of tropical and extratropical mean  
357 RCTT and AoA from the simple Lagrangian model agree reasonably well with the results  
358 from the GCM (Fig. 6), and so does the distribution of "aging by mixing" (Fig. 5c). The  
359 Lagrangian model broadly reproduces the mean latitudinal distribution of AoA and aging  
360 by mixing (Fig. 7), even though the maximum in aging by mixing is shifted by about  
361  $10^\circ$  poleward compared to the GCM. Since the Lagrangian model is a very simplified  
362 representation of transport through the stratosphere, an exact quantitative replication of

363 AoA in the GCM should not be expected. However, general qualitative features of aging  
364 by mixing are well captured. Therefore, we can use this idealized model to improve the  
365 conceptual understanding of the effects mixing at different locations can have on AoA.

366 Fig. 5 contrasts aging by mixing from the full integration to cases in which mixing is  
367 applied 1) only within the tropics and the extratropics (Fig. 5d) and 2) only between the  
368 tropics and extratropics (Fig. 5e). As discussed in Sec. 4.2.1, mixing within the extra-  
369 tropics has a strong local effect and flattens the age gradient, but tropical-extratropical  
370 mixing causes an increase in AoA in the entire stratosphere above the level of mixing.  
371 Mixing within the tropics has almost no effect, as the gradient in RCTT is small in the  
372 tropics. In the mean over all air parcels (“global mean”), AoA increases from 1.25 to 1.69  
373 years between the case without mixing and the full integration (Table 1). This increase is  
374 almost entirely caused by tropical-extratropical mixing, while mixing within the tropics  
375 and extratropics has a minor effect, both in the global mean (Table 1, cases  $\mu_{TrEx} = 0$   
376 and  $\mu_{Ex}, \mu_{Tr} = 0$ ), and for tropical and extratropical mean profiles (Fig. 8). The increase  
377 of global mean AoA would be even higher by about 35% if in-mixing of tropospheric air  
378 in the lowermost stratosphere is neglected, as verified by an integration in which tropical-  
379 extratropical mixing below the tropical tropopause is set to zero ( $\mu_{tropo} = 0$  in Table 1  
380 and Fig. 8).

381 Mixing within the extratropics does, however, affect the latitudinal distribution of aging  
382 by mixing. As shown in Fig. 7, aging by mixing is nearly constant at all latitudes for the  
383 case with only mixing across the subtropical barrier, consistent with the prediction by the  
384 TLP model. Only when including mixing within the extratropics, the maximum of aging  
385 by mixing in mid-latitudes, and the negative values at high latitudes can be reproduced

386 by the Lagrangian model. Since the tropical and extratropical mean profiles are, however,  
387 not affected by mixing within those regions, applying the TLP model equations to the  
388 mean profiles from the GCM appears to be a valid approach.

389 The role of mixing at different heights is further examined by integrations in which  
390 tropical-extratropical mixing is only permitted below or above 500 K. The global AoA  
391 increase is far larger for mixing at lower altitudes than for mixing above 500 K (Table 1).  
392 Since mixing at a certain level affects AoA only above this level, it can be expected that  
393 mixing at lower levels results in an overall greater response in AoA.

394 The findings with the simple Lagrangian random walk model suggest that the distribu-  
395 tion of aging by mixing in the GCM may be explained as follows: the decrease of AoA  
396 in the lowermost stratosphere is caused by in-mixing of tropospheric air. The decrease at  
397 high latitudes above about 100 hPa, on the other hand, results from mixing within the  
398 extratropics, that flattens the gradient in AoA. The general increase in AoA due to mixing  
399 is caused by mixing between tropics and extratropics. Tropical-extratropical mixing at a  
400 certain levels affects AoA above this level – or, to put it the other way round, AoA at a  
401 certain level is influenced by mixing at all levels below. Thus, the higher up, the more  
402 mixing levels can contribute to aging by mixing. Therefore, aging by mixing increases  
403 with height.

## 5. Coupling of mixing and residual transport

### 5.1. Mixing Efficiency in the GCM for different climate states

404 The residual circulation is mechanically driven by the momentum deposition of breaking  
405 waves [*Haynes et al.*, 1991]. These are represented in GCMs both by resolved planetary  
406 and synoptic scale waves and by parametrized small scale gravity waves. The two-way

407 mixing mass flux can as well be expected to be linked to wave breaking, that results in  
 408 strong stirring [*Haynes and Shuckburgh, 2000*]. As discussed in the last section, AoA is  
 409 controlled both by the residual circulation and by the strength of the two-way mixing  
 410 mass flux. However, as the two processes are known not to be independent, we want to  
 411 investigate in this section how they are coupled. To this end, we compare three equilibrium  
 412 climate states in the model, representative of the mean climate in the 1860s, the 1990s  
 413 and the 2050s.

414 The residual circulation (measured by tropical mean  $\bar{w}^*$ ) is slightly enhanced in 1990  
 415 compared to 1860, and even more so in 2050 (Fig. 9 left). Consequently, RCTT decreases  
 416 from 1860 to 2050, and so does AoA (Fig. 9 right). In Fig. 10, mean tropical AoA at  
 417 20 hPa is plotted against mean tropical RCTT for the three simulations. This Figure  
 418 shows not only that AoA and RCTT both decrease in a warmer climate, but also that  
 419 the ratio AoA/RCTT remains approximately constant (i.e. they lie on a straight line  
 420 extending through zero). Thus, mixing amplifies changes in AoA, with an about twice  
 421 as large decrease in AoA than in RCTT both for the difference between the TS1860 and  
 422 TS1990 simulations and between TS1990 and TS2050. In other words, the relative aging  
 423 of air by mixing remains approximately constant.

424 For the solution of the TLP model with a height-independent vertical velocity  $w_T$ , the  
 425 ratio AoA to RCTT equals  $\Gamma_T^\epsilon/\Gamma_T^0 = 1 + \epsilon(1 + \frac{1}{\alpha})$  (see Equ. 6), which depends only on the  
 426 mixing efficiency  $\epsilon$ . The nearly constant ratio therefore indicates that the mixing efficiency  
 427 does not change between the simulations. This is confirmed when deriving the mixing  
 428 efficiency from the profiles of AoA and RCTT for the solution with height-depended  $w_T(z)$   
 429 as best fit (as in Sec. 4.1): For all three climate states a mixing efficiency of  $\epsilon = 0.32$  is

430 obtained. The TLP model with this mixing efficiency describes the change in AoA and  
 431 RCTT between the climate states well (within 10% at all levels).

432 The mixing efficiency  $\epsilon$  is defined as the ratio of the two-way mixing mass flux to the  
 433 net mass flux. Thus, a constant  $\epsilon$  for all three climate states corresponds to changes in  
 434 the two-way mixing mass flux that are proportional to those in the net mass flux. In  
 435 other words, the results indicate that stronger wave driving of the residual circulation,  
 436 that drive the enhanced net mass flux [*Bunzel and Schmidt, 2013*], causes more two-way  
 437 mixing that results in an equally strong enhancement in the two-way mixing mass flux.

438 Overall, the nearly constant mixing efficiency is equivalent to nearly constant relative  
 439 aging by mixing. Thus, the decrease in absolute aging by mixing is entirely driven by the  
 440 strengthened residual circulation: Aging by mixing is indirectly proportional to the resid-  
 441 ual circulation strength (measured by  $\bar{w}^*$ ; see Equ. 8). The stronger residual circulation  
 442 also causes the recirculation to speed up: the additional transit time an air parcels ages  
 443 while recirculating is reduced. In other words, the decrease in AoA due to the increase in  
 444 the residual circulation is amplified by mixing effects, that are, according to this study,  
 445 tightly coupled to the residual circulation changes.

## 5.2. PV gradients

Insight into the relation between the wave forcing, residual circulation strength, and  
 mixing strength can be gained by considering the transformed Eulerian mean zonal mo-  
 mentum equation. In isentropic coordinates, the zonal momentum equation for adiabatic,  
 inviscid flow under steady state, can be written as [derived from Equ. 3.9.9 in *Andrews*  
*et al.*, 1987; *Plumb*, 2002]:

$$-\bar{v}^* \bar{P}^* = \overline{\hat{v} \hat{P}^*} \quad (10)$$

446 Here,  $v$  is the meridional velocity on isentropic levels, and  $P$  the PV.  $\bar{x}^*$  denotes the zonal  
 447 average weighted by the isentropic density, and  $\hat{x}$  the deviation from  $\bar{x}^*$ . According to  
 448 this relation, transport of mean PV by the zonal mean circulation is balanced by eddy  
 449 fluxes of PV.

Using a flux-gradient relationship for the eddy PV flux, i.e.  $\overline{\hat{v}\hat{P}^*} = -K_{mix}\bar{P}_y^*$  (with  
 diffusivity coefficient  $K_{mix}$ ), we obtain

$$\bar{v}^*\bar{P}^* = K_{mix}\bar{P}_y^* \quad (11)$$

Furthermore, by setting the Diffusivity to a mixing velocity scale times a horizontal mixing  
 length scale ( $K_{mix} \sim \overline{v_{mix}} * L$ ), the ratio of the diffusive, or “mixing” velocity to the mean  
 meridional velocity is given by

$$\frac{\overline{v_{mix}}}{\bar{v}^*} \sim \frac{1}{L} \frac{\bar{P}^*}{\bar{P}_y^*} \quad (12)$$

450 Thus, the ratio of mean PV to the meridional PV gradient is a measure of the relative  
 451 role of mixing and mean transport (for a given horizontal mixing length scale). Larger  
 452 ratios indicate a more important role of mixing, while relatively small values indicate  
 453 that mean transport dominates. The climatological mean ratio of mean PV to the PV  
 454 gradient, scaled by the earth radius for the TS1990 simulation is shown in Fig. 11 (top).  
 455 We find elevated ratios between about 30° to 60°N/S above 400 K, consistent with strong  
 456 wave mixing in the surf zones. The ratio decreases towards the tropics, where the zonal  
 457 wind approaches zero and wave propagation is largely prohibited. Minima in the ratio at  
 458 around 60°N/S mark the barrier formed by the polar vortex, in particular in the SH. At  
 459 high latitudes the ratio of mean PV to the PV gradient increases strongly, reflecting that  
 460 the mean meridional velocity is close to zero here.

461 The relative changes in the ratio of mean PV to the PV gradient between the TS1860 to  
 462 the TS1990 simulations, and the TS1990 to TS2050 simulations are shown in the middle  
 463 and bottom panel of Fig. 11. From 1860 to 1990, the Antarctic polar vortex strengthens,  
 464 and thus the ratio decreases, as a stronger vortex more strongly suppresses wave mixing.  
 465 This decrease in mixing is reflected in a stronger gradient in AoA (not shown). From 1860  
 466 to 1990, the ratio decreases by about 10-15% at latitudes between about 30-50°N/S, and  
 467 this decrease is even stronger (up to 30%) from 1990 to 2050. This decrease in the relative  
 468 strength of mixing appears to be associated with the strengthening of the subtropical jets,  
 469 which are marked by strong PV gradients.

470 The results of the last section imply that the mixing mass flux between tropics and  
 471 extratropics changes proportionally to mean meridional transport in the three equilibrium  
 472 climate states. According to Equ. 12, we should thus expect that the ratio of mean PV to  
 473 the PV gradient between tropics and extratropics remains close to constant. As in the TLP  
 474 model, we set the boundaries between tropics and extratropics at 30°N/S. The horizontal  
 475 mixing length scale  $L$  is then the mean mixing length between tropics and extratropics,  
 476 and the PV gradient is  $\bar{P}_y^* = \Delta\bar{P}^*/L$ , where  $\Delta\bar{P}^*$  is the extratropical - tropical PV  
 477 difference. Therefore, the relation of the mixing velocity to the mean meridional velocity  
 478 across the tropical boundaries can be approximated by the tropical mean PV to the  
 479 extratropical-tropical PV difference.

480 This ratio is shown for the three climate states simulated by the GCM in Fig. 12. Above  
 481 400 K, the ratio differs by less than 3% between the three climate states. At 400 K, the  
 482 ratio decreases by 8% from 1860 to 1990 and by 17% from 1990 to 2050. This decrease in  
 483 the PV ratio across 30°N/S is consistent with the decline in  $\bar{P}^*/\bar{P}_y^*$  around the subtropical

484 jets shown in Fig. 11. Above 400 K, changes in  $\bar{P}^*/\bar{P}_y^*$  occur away from the subtropical  
485 barrier, so that exchange of air between tropics and extratropics is not affected.

486 The scaling arguments using PV gradients therefore largely support the results of the  
487 last section: Between 450-550 K (i.e. about 65-35 hPa), the relative role of mixing versus  
488 mean transport across the subtropical barrier as estimated by the ratio of mean PV to PV  
489 gradient remain close to constant, despite changes in the meridional circulation. However,  
490 we found a decrease in the relative role of mixing at 400 K, which might be related to a  
491 strengthening of the subtropical jets. We would expect this decrease to be reflected in  
492 AoA, in particular since mixing just above the tropopause was found to contribute most  
493 to aging by mixing (Sec. 4.2). However, the changes at 400 K appear to be unimportant  
494 for the mixing efficiency, which is derived with the TLP model as best fit over the entire  
495 lower stratosphere. Note, however, that deviations between the TLP fit with a mixing  
496 efficiency of 0.32 and the AoA from the GCM are largest just above the tropopause (see  
497 Fig. 3).

## 6. Discussion and Conclusions

498 The conceptual picture of stratospheric transport consisting of net transport along the  
499 residual circulation and modifications by a two-way mass flux (“mixing mass flux”) is used  
500 widely in stratospheric research [e.g. *Plumb*, 2002]. Here, the diagnostic “aging by mix-  
501 ing” is introduced that quantifies the effects of mixing on age of air. This aging by mixing  
502 is obtained by differencing AoA with a hypothetical age that would result from transport  
503 along the residual circulation only, the residual circulation transit time (RCTT). Aging  
504 by mixing is calculated from global model data, and the processes that lead to aging by  
505 mixing are investigated with conceptual model approaches, namely with a tropical leaky

506 pipe model and a simple Lagrangian random walk model. Above the tropical tropopause,  
507 mixing between the tropics and extratropics causes air to recirculate along the residual  
508 circulation, thereby enhancing AoA above the level at which mixing occurs. In the lower-  
509 most stratosphere AoA is reduced by mixing with tropospheric air, which adds very young  
510 air and removes old air from the stratosphere. Using the Lagrangian model, we showed  
511 that mixing within the extratropics is necessary to explain the latitudinal distribution of  
512 aging by mixing (which maximizes in mid-latitudes), but has a negligible (despite non-  
513 zero) impact on extratropical mean AoA. Therefore, tropical and extratropical mean AoA  
514 profiles from the GCM can be approximated with the tropical leaky pipe model equations,  
515 which only consider the effects of mixing across the subtropical barrier.

516 Decreases of AoA in a future climate are both due to a decrease in RCTT and in aging  
517 by mixing, each contributing about half. This result is consistent with *Li et al.* [2012],  
518 who examined changes in age spectra and showed that the tail of the spectrum contributes  
519 significantly to the future decrease in mean AoA.

520 Fitting a simple tropical leaky pipe model to AoA from the global model for different  
521 climate equilibrium states suggests that the strength of the two-way mixing mass flux is  
522 tightly coupled to the net or residual mass flux, so that their ratio (the mixing efficiency)  
523 remains close to constant. Thus, the relative aging of air by mixing remains approximately  
524 constant. The decrease in absolute aging by mixing is not caused by a decrease in mixing,  
525 but by the stronger residual circulation, which leads to faster recirculation. This is again  
526 consistent with the decrease in the tail of the spectrum, and in particular with strong  
527 correlations of tail decay time scales with the strength of tropical upwelling found by  
528 *Li et al.* [2012]. Furthermore, *Li et al.* [2012] found that mixing strength (estimated as

529 equivalent length from  $\text{N}_2\text{O}$ ) increases proportionally with tropical upwelling, consistent  
530 with our finding of a constant mixing efficiency.

531 We further verified the result of a nearly constant mixing efficiency by evaluating the  
532 ratio between mean PV to the PV gradient between tropics and extratropics, that is  
533 a measure of the relative roles of mixing versus mean horizontal transport. In most  
534 of the lower stratosphere, this ratio is found to remain close to constant between the  
535 climate states, consistent with a constant mixing efficiency. However, just above the  
536 tropopause (at 400 K) the ratio of mean PV to PV gradients decreases, indicating that  
537 mixing fluxes decrease relative to mean transport. An increase in the strength of the  
538 subtropical jets might cause this decrease in mixing relative to mean transport. The causes  
539 for the decrease in the relative strength of mixing at 400 K indicated by the PV analysis,  
540 along with deviations in the TLP model fits at these levels remain to be identified. It might  
541 indicate a different regime of transport and mixing in the shallow branch. However, note  
542 that both the TLP model and the PV scaling arguments rely on simplified assumptions.  
543 Independent measures of mixing like the effective diffusivity [*Allen and Nakamura, 2001*],  
544 or Lagrangian measures, have to be used to verify the relation of the two-way mass flux to  
545 residual transport (as shown in *Li et al. [2012]*). Furthermore, it is questionable whether  
546 the tight coupling between residual transport and mixing also holds at higher altitudes  
547 where gravity waves play a larger role in driving the residual circulation, since gravity  
548 waves mostly cause two-way mixing in the vertical [*Grygalashvily et al., 2012*], but do not  
549 primarily alter the PV distribution along isentropes in the same manner as Rossby waves.

550 The modeled strength of the two-way mass flux depends on stirring by large-scale winds,  
551 but also on the advection scheme and representation of (sub-grid scale) diffusion. There-

552 fore, the two-way mass flux likely differs between models, even if the large-scale dynamics  
553 are similar, resulting in differences in the mixing efficiency. The separation of AoA into  
554 RCTT and aging by mixing, and the comparison of the relative aging by mixing (or of  
555 the mixing efficiency) between models might provide a helpful tool to identify causes for  
556 model deficits in the simulation of AoA, that are widely found in state-of-the art global  
557 models [see Chapter 5 of *SPARC-CCMVal*, 2010].

558 An as yet unresolved puzzle is the discrepancy between the few available observational  
559 records of the temporal development of AoA over the last decades and modeled changes  
560 in AoA. Global models simulate an increase in the BDC and associated decrease in AoA  
561 over the last decades and in the future [*Butchart et al.*, 2010]. The longest available time  
562 series of AoA derived from measurements of  $SF_6$  shows no significant change in AoA at  
563 northern mid-latitudes at around 25 km [*Engel et al.*, 2009]. This results is backed up by  
564 AoA records derived from satellite observations of  $SF_6$  [*Stiller et al.*, 2012], and by AoA  
565 time series calculated from reanalysis [*Diallo et al.*, 2012]. The latter study suggests that  
566 AoA decreased in the lower stratosphere, but increased above about 20 to 25 km over the  
567 period 1989-2010. On the basis of tracer measurements in the lowermost stratosphere  
568 and residual circulation transit time calculations, *Bönisch et al.* [2011] suggested that  
569 structural changes in the BDC occurred over the last decades, with an intensification of  
570 the shallow branch, while the deep branch remained unchanged.

571 How structural changes in the residual circulation would modify AoA can be illustrated  
572 with the Lagrangian random walk model used in this study. The Lagrangian model  
573 allows for a separation of the shallow and deep branch, and the response to a hypothetical  
574 speed up of the shallow branch with associated increases in the mixing fraction (given

575 a constant mixing efficiency) are shown in Fig. 13. The faster circulation in the lower  
576 stratosphere causes decreases in AoA there, but above, AoA increases. This increase is  
577 due to aging by mixing, which, as discussed above, results from an enhanced mixing mass  
578 flux in the lower stratosphere. This simple experiment shows that despite the coupling of  
579 mixing and the residual circulation, mixing can act to either amplify or dampen residual  
580 circulation changes, depending on the relative location in the atmosphere with respect to  
581 the circulation changes. The AoA changes due to a shallow branch enhancement found  
582 in the Lagrangian model experiment are consistent with the findings by *Bönisch et al.*  
583 [2011] and the AoA trend pattern in reanalysis data presented by *Diallo et al.* [2012].

### Appendix A: Parameter settings in the Lagrangian random walk model

584 The simple Lagrangian random walk model used in Sec. 4.2 advects air parcels along  
585 trajectories that are calculated from residual velocities. Two-way mixing is realized by  
586 exchanging a certain fraction of air parcels between or within different groups, namely  
587 the tropics (region of upwelling) and the extra-tropics (region of downwelling). The air  
588 parcels are randomly selected according to an uniform distribution. The points where this  
589 parcel exchange (=mixing) is performed are located on the intersections of trajectories  
590 with selected isentropic levels. Several different parameters need to be chosen:

- 591 1. Number of trajectories (Ntraj)
- 592 2. Number of theta levels (TL) on which mixing is performed
- 593 3. The fraction of air parcels that are exchanged (mixing fraction  $\mu$ )

594 For the “base case”, we use monthly mean residual velocities to calculate 20 trajectories  
 595 that are initialized at the tropopause between 40 and 85°N, and 20 mixing levels between  
 596 340 to 2000 K.

The fraction of mass exchange representing mixing within the extratropics and within the tropics is set to 0.25. The choice of the fraction of air exchange between the tropics and the extratropics ( $\mu_{TrEx}(z)$ ) is anticipated to be based on physical principles. In particular, we assume that the net mass flux from the tropics to the extratropics is proportional to the mixing mass flux, as suggested by the results of Sec. 5. Thus,

$$\epsilon * massflux_{net} = massflux_{mix} \quad (A1)$$

where  $\epsilon$  is the mixing efficiency as defined in the TLP model. The net mass flux from the tropics to the extratropics in one hemisphere can be expressed as:

$$massflux_{net} = -\frac{1}{2} \frac{\partial}{\partial z} (M_T w_T) = -\frac{1}{2} \frac{\partial}{\partial z} \left( M_T(z_T) \exp\left(-\frac{z-z_T}{H}\right) w_T(z) \right) \quad (A2)$$

assuming an increase of the mass  $M_T$  with height according to  $M_T(z) = M_T(z_T) \exp\left(-\frac{z-z_T}{H}\right)$ , where  $M_T(z_T)$  is the mass at the tropical tropopause. The mixing mass flux in the Lagrangian model can be written as:

$$massflux_{mix} = \mu_{TrEx}(z) * 100m_0 N(z) \frac{1}{\Delta t} \quad (A3)$$

597 where  $m_0$  is the mass of one air parcel that travels along the trajectories, and  $N$  is the  
 598 number of trajectories that take part in the mixing process at level  $z$ .  $\Delta t$  is the time step  
 599 of the Lagrangian model, here 5 days.

Combining these Equations, one obtains for the mixing fraction  $\mu_{TrEx}(z)$ :

$$\mu_{TrEx}(z) = -\epsilon \frac{0.5M_T(z_T)}{100m_0 N(z)} * \Delta t * \frac{\partial}{\partial z} \left( \exp\left(-\frac{z-z_T}{H}\right) w_T(z) \right). \quad (A4)$$

Given that the total mass at the tropical tropopause equals the mass of the air parcels that are located at this level in the Lagrangian model, i.e.  $2 * 100 * m_0 * N(z_T)$ , we can write:

$$\mu_{TrEx}(z) = -\epsilon \frac{N(z_T)}{N(z)} * \Delta t * \frac{\partial}{\partial z} \left( \exp\left(-\frac{z - z_T}{H}\right) w_T(z) \right). \quad (\text{A5})$$

600 Since mixing is performed on a finite number of height levels,  $\mu$  needs to be scaled to  
 601 represent mixing over the entire layer it represents. Thus, the fraction of parcels mixed  
 602 (exchanged) at level  $z$  is multiplied by the mass within the entire layer divided by the  
 603 mass at level  $z$ :  $\mu_{TrEx}(\Delta z) = \mu_{TrEx}(z) * N(\Delta z)/N(z)$ . This ensures robust results with  
 604 respect to the location and number of mixing levels. As shown in Table 2, global mean  
 605 age simulated with additional levels (37 instead of 20 used in the base case) differs by less  
 606 than 1% from the base case.

607 The tropical vertical velocity  $w_T$  used here is the the tropical mean ( $30^\circ\text{N/S}$ )  $\bar{w}^*$  taken  
 608 from the GCM data. The mixing efficiency  $\epsilon$  can be derived from the relation of AoA  
 609 and RCTT in the GCM by using the TLP model (see Sec. 4.1). For the latitude band  
 610 of  $30^\circ\text{N}-30^\circ\text{S}$ , the TLP fit gives  $\epsilon \approx 0.3$ . This value gives good agreement between the  
 611 Lagrangian calculations and the AoA profiles from the GCM (see Fig. 6). Calculations  
 612 with modified values of  $\epsilon$  show that AoA increases in the global mean for higher  $\epsilon$ , as  
 613 expected (see Table 2).

614 When using a different number of trajectories, different global mean values of RCTTs  
 615 are obtained, as listed in Table 2. Applying mixing in the same manner to those cases  
 616 results in an increase in global mean AoA in all cases, and tropical and extratropical  
 617 profiles show good agreement (not shown). However, in the case of using 10 trajectories,  
 618 AoA increases by 40% due to mixing, while when using 40 trajectories the increase lies

619 around 30%. The base case gave a 35% increase. Thus, the simple Lagrangian model  
620 is somewhat sensitive to the choice of the trajectory set, and it should be regarded as a  
621 conceptual model used to highlight different effects rather than a quantitative model.

622 **Acknowledgments.** This study was funded by the Deutsche Forschungsgemeinschaft  
623 (DFG) through the DFG-research group SHARP (Stratospheric Change And its Role for  
624 climate Prediction). We thank M. Dameris, V. Grewe and M. Abalos for discussion and  
625 comments, as well as R. A. Plumb and the two anonymous reviewer for very valuable  
626 comments on the manuscript. TB acknowledges funding through the Climate and Large-  
627 Scale Dynamics Program of the U.S. National Science Foundation.

## References

- 628 Allen, D. R., and N. Nakamura (2001), A seasonal climatology of effective diffusivity in  
629 the stratosphere, *J. Geophys. Res.*, *106*, 7917–7936, doi:10.1029/2000JD900717.
- 630 Andrews, D., J. Holton, and C. Leovy (1987), *Middle Atmosphere Dynamics*, Academic  
631 Press, San Diego, California.
- 632 Austin, J., and F. Li (2006), On the relationship between the strength of the Brewer-  
633 Dobson circulation and the age of stratospheric air, *Geophys. Res. Lett.*, *33*, 17,807,  
634 doi:10.1029/2006GL026867.
- 635 Birner, T., and H. Bönisch (2011), Residual circulation trajectories and transit times  
636 into the extratropical lowermost stratosphere, *Atmos. Chem. Phys.*, *11*(7), 817–827,  
637 doi:doi:10.5194/acp-11-817-2011.
- 638 Bunzel, F., and H. Schmidt (2013), The brewer-dobson circulation in a changing cli-  
639 mate: Impact of the model configuration, *J. Atmos. Sci.*, *70*, 1437–1455, doi:doi:

- 640 <http://dx.doi.org/10.1175/JAS-D-12-0215.1>.
- 641 Butchart, N., I. Cionni, V. Eyring, D. W. Waugh, H. Akiyoshi, J. Austin, C. Bruehl, M. P.  
642 Chipperfield, E. Cordero, M. Dameris, R. Deckert, S. M. Frith, R. R. Garcia, A. Gettel-  
643 man, M. A. Giorgetta, D. E. Kinnison, F. Li, E. Manzini, C. McLandress, S. Pawson,  
644 G. Pitari, E. Rozanov, F. Sassi, T. G. Shepherd, K. Shibata, and W. Tian (2010),  
645 Chemistry-climate model simulations of twenty-first century stratospheric climate and  
646 circulation changes, *J. Clim.*, *23*, 5349–5374, doi:10.1175/2010JCLI3404.1.
- 647 Butchart (2014), The Brewer-Dobson Circulation, *Rev. Geophys.*, accepted, doi:  
648 10.1002/2013RG000448.
- 649 Bönisch, H., A. Engel, J. Curtius, T. Birner, and P. Hoor (2009), Quantifying transport  
650 into the lowermost stratosphere using simultaneous in-situ measurements of sf6 and co2,  
651 *Atmos. Chem. Phys.*, *9*, 5905–5919, doi:doi:10.5194/acp-9-5905-2009.
- 652 Bönisch, H., A. Engel, T. Birner, P. Hoor, D. W. Tarasick, and E. A. Ray (2011), On the  
653 structural changes in the brewer-dobson circulation after 2000, *Atmos. Chem. Phys.*,  
654 *11*, 3937–3948, doi:doi:10.5194/acp-11-3937-2011.
- 655 Calvo, N., and R. R. Garcia (2009), Wave Forcing of the Tropical Upwelling in the Lower  
656 Stratosphere under Increasing Concentrations of Greenhouse Gases, *J. Atmos. Sci.*, *66*,  
657 3184–3196, doi:10.1175/2009JAS3085.1.
- 658 Diallo, M., B. Legras, and A. Chdin (2012), Age of stratospheric air in the era-interim,  
659 *Atmos. Chem. Phys.*, *12*, 12,133–12,154, doi:doi:10.5194/acp-12-12133-2012.
- 660 Engel, A., T. Mobius, H. Bonisch, U. Schmidt, R. Heinz, I. Levin, E. Atlas, S. Aoki,  
661 T. Nakazawa, S. Sugawara, F. Moore, D. Hurst, J. Elkins, S. Schauffler, A. Andrews,  
662 and K. Boering (2009), Age of stratospheric air unchanged within uncertainties over

- 663 the past 30 years, *Nature Geoscience*, *2*, 28 – 31, doi:doi:10.1038/ngeo388.
- 664 Garcia, R., and W. Randel (2008), Acceleration of the brewerdobson circulation due to  
665 increases in greenhouse gases, *J. Atmos. Sci.*, *65*, 27312739.
- 666 Grygalashvyly, M., E. Becker, and G. R. Sonnemann (2012), Gravity wave mixing and  
667 effective diffusivity for minor chemical constituents in the mesosphere/lower thermo-  
668 sphere, *Space Sci. Rev.*, *168*, 333–362, doi:doi:10.1007/s11214-011-9857-x.
- 669 Hall, T. M., and R. Plumb (1994), Age as a diagnostic of stratospheric transport, *J.*  
670 *Geophys. Res.*, *99*, 1059 1070.
- 671 Haynes, P., and E. Shuckburgh (2000), Effective diffusivity as a diagnostic of at-  
672 mospheric transport 1. stratosphere, *J. Geophys. Res.*, *105*, 22,777–22,794, doi:  
673 10.1029/2000JD900093.
- 674 Haynes, P., C. Marks, M. McIntyre, T. Shepherd, and K. Shine (1991), On the 'downward  
675 control' of extratropical diabatic circulations by eddy-induced mean zonal forces, *J.*  
676 *Atmos. Sci.*, *48*(4), 651–678.
- 677 Li, F., D. Waugh, A. R. Douglass, P. A. Newman, S. E. Strahan, J. Ma, J. E. Nielsen, and  
678 Q. Liang (2012), Long-term changes in stratospheric age spectra in the 21st century in  
679 the goddard earth observing system chemistry-climate model (geosccm), , 117, d20119,,  
680 *J. Geophys. Res.*, *117*, D20,119, doi:doi:10.1029/2012JD017905.
- 681 Marsland, S. (2003), The max-planck-institute global ocean/sea ice model with or-  
682 thogonal curvilinear coordinates, *Ocean Modell.*, *5*, 91–127, doi:doi:10.1016/S1463-  
683 5003(02)00015-X.
- 684 McIntyre, M., and T. Palmer (1984), The 'surf zone' in the stratosphere, *Journal of*  
685 *Atmospheric and Terrestrial Physics*, *46*(9), 825–849.

- 686 McLandress, C., and T. G. Shepherd (2009), Simulated Anthropogenic Changes in the  
687 Brewer-Dobson Circulation, Including Its Extension to High Latitudes, *J. Clim.*, *22*,  
688 1516–1540, doi:10.1175/2008JCLI2679.1.
- 689 Nakicenovic, N., and R. Swart (2000), Special report on emissions scenarios, *Tech. rep.*,  
690 Cambridge University Press.
- 691 Neu, J. L., and R. A. Plumb (1999), Age of air in a "leaky pipe" model of stratospheric  
692 transport, *J. Geophys. Res.*, *104(D16)*, 243–255, doi:doi:10.1029/1999JD900251.
- 693 Oberländer, S., U. Langematz, and S. Meul (2013), Unraveling impact factors for fu-  
694 ture changes in the brewer-dobson circulation, *Journal of Geophysical Research: Atmo-*  
695 *spheres*, *118*, 10,296–10,312.
- 696 Okamoto, K., K. Sato, and H. Akiyoshi (2011), A study on the formation and  
697 trend of the brewer-dobson circulation, *J. Geophys. Res.*, *116(D10)*, D10, doi:  
698 10.1029/2010JD014953.
- 699 Plumb, R. (2002), Stratospheric transport, *Journal of the Meteorological Society of Japan*,  
700 *80*, 793–809.
- 701 Randel, W., J. Gille, A. Roche, J. Kumer, J. Mergenthaler, J. Waters, E. Fishbein,  
702 and W. Lahoz (1993), Stratospheric transport from the tropics to middle latitudes by  
703 planetary-wave mixing, *Nature*, *365*, 533–535.
- 704 Ray, E. A., F. L. Moore, K. H. Rosenlof, S. M. Davis, H. Bönisch, O. Morgenstern,  
705 D. Smale, E. Rozanov, M. Hegglin, G. Pitari, E. Mancini, P. Braesicke, N. Butchart,  
706 S. Hardiman, F. Li, K. Shibata, and D. A. Plummer (2010), Evidence for changes  
707 in stratospheric transport and mixing over the past three decades based on multiple  
708 datasets and tropical leaky pipe analysis, *J. Geophys. Res.*, *115*, D21,304.

- 709 Röckner, E., G. Bäuml, L. Bonaventura, R. Brokopf, M. Esch, M. Giorgetta, S. Hagemann,  
710 I. Kirchner, L. Kornbluh, E. Manzini, A. Rhodin, U. Schlese, U. Schulzweida, and  
711 A. Tompkins (2003), The atmospheric general circulation model echam 5. part i: Model  
712 description, *Tech. rep.*, Max Planck Institute for Meteorology Rep. 349.
- 713 Shepherd, T., and C. McLandress (2011), A robust mechanism for strengthening of the  
714 brewer-dobson circulation in response to climate change: critical-layer control of sub-  
715 tropical wave breaking, *J. Atmos. Sci.*, *68*, 784–797.
- 716 Shepherd, T. G. (2007), Transport in the middle atmosphere, *J. Meteor. Soc. Japan*, *85B*,  
717 165–191.
- 718 Shuckburgh, E., and P. Haynes (2003), Diagnosing transport and mixing using a tracer-  
719 based coordinate system, *Physics of Fluids*, *15*, 3342–3357, doi:10.1063/1.1610471.
- 720 SPARC-CCMVal (2010), Sparc report on the evaluation of chemistry-climate models, v.  
721 eyring, t. g. shepherd, d. w. waugh (eds.), sparc report no. 5, *Tech. Rep. SPARC Report*  
722 *No. 5*, WCRP-132, WMO/TD-No. 1526.
- 723 Sparling, L. C., J. A. Kettleborough, P. H. Haynes, M. E. McIntyre, J. E. Rosenfield,  
724 M. R. Schoeberl, and P. A. Newman (1997), Diabatic cross-isentropic dispersion in the  
725 lower stratosphere, *J. Geophys. Res.*, *102*, 25,817–25,829.
- 726 Stevens, B., M. Giorgetta, M. Esch, T. Mauritsen, T. Crueger, S. Rast, M. Salz-  
727 mann, H. Schmidt, J. Bader, K. Block, R. Brokopf, I. Fast, S. Kinne, L. Kornbluh,  
728 U. Lohmann, R. Pincus, T. Reichler, and E. Roeckner (2013), Atmospheric component  
729 of the mpi-m earth system model: Echam6, *Journal of Advances in Modeling Earth*  
730 *Systems*, *5*, 146–172, doi:doi:10.1002/jame.20015.

- 731 Stiller, G. P., T. von Clarmann, F. Haanel, B. Funke, N. Glatthor, U. Grabowski, S. Kell-  
732 mann, M. Kiefer, A. Linden, S. Lossow, and M. Lopez-Puertas (2012), Observed tempo-  
733 ral evolution of global mean age of stratospheric air for the 2002 to 2010 period, *Atmos.*  
734 *Chem. Phys.*, *12*, 3311–3331, doi:doi:10.5194/acp-12-3311-2012.
- 735 Strahan, S. E., M. R. Schoeberl, and S. D. Steenrod (2009), The impact of tropical recir-  
736 culation of polar composition, *Atmos. Chem. Phys.*, *9*, 2471–2480, doi:doi:10.5194/acp-  
737 9-2471-2009.
- 738 Trepte, C. R., and M. H. Hitchman (1992), Tropical stratospheric circulation deduced  
739 from satellite aerosol data, *Nature*, *355*, 626–628.
- 740 Vuuren, D. P., J. Edmonds, M. Kainuma, K. Riahi, A. Thomson, K. Hibbard, G. C.  
741 Hurtt, T. Kram, V. Krey, J.-F. Lamarque, T. Masui, M. Meinshausen, N. Nakicenovic,  
742 S. J. Smith, and S. K. Rose (2011), The representative concentration pathways: An  
743 overview, *Climatic Change*, *109*, 5–31.

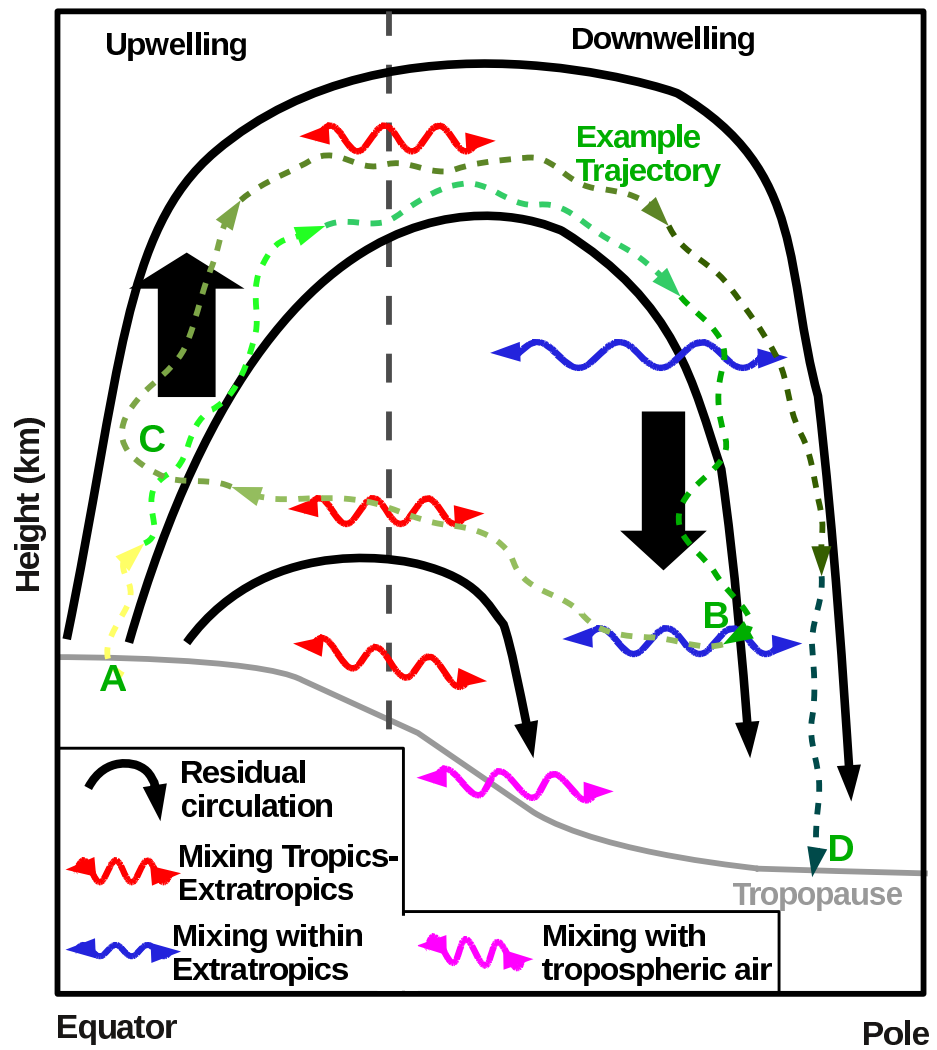
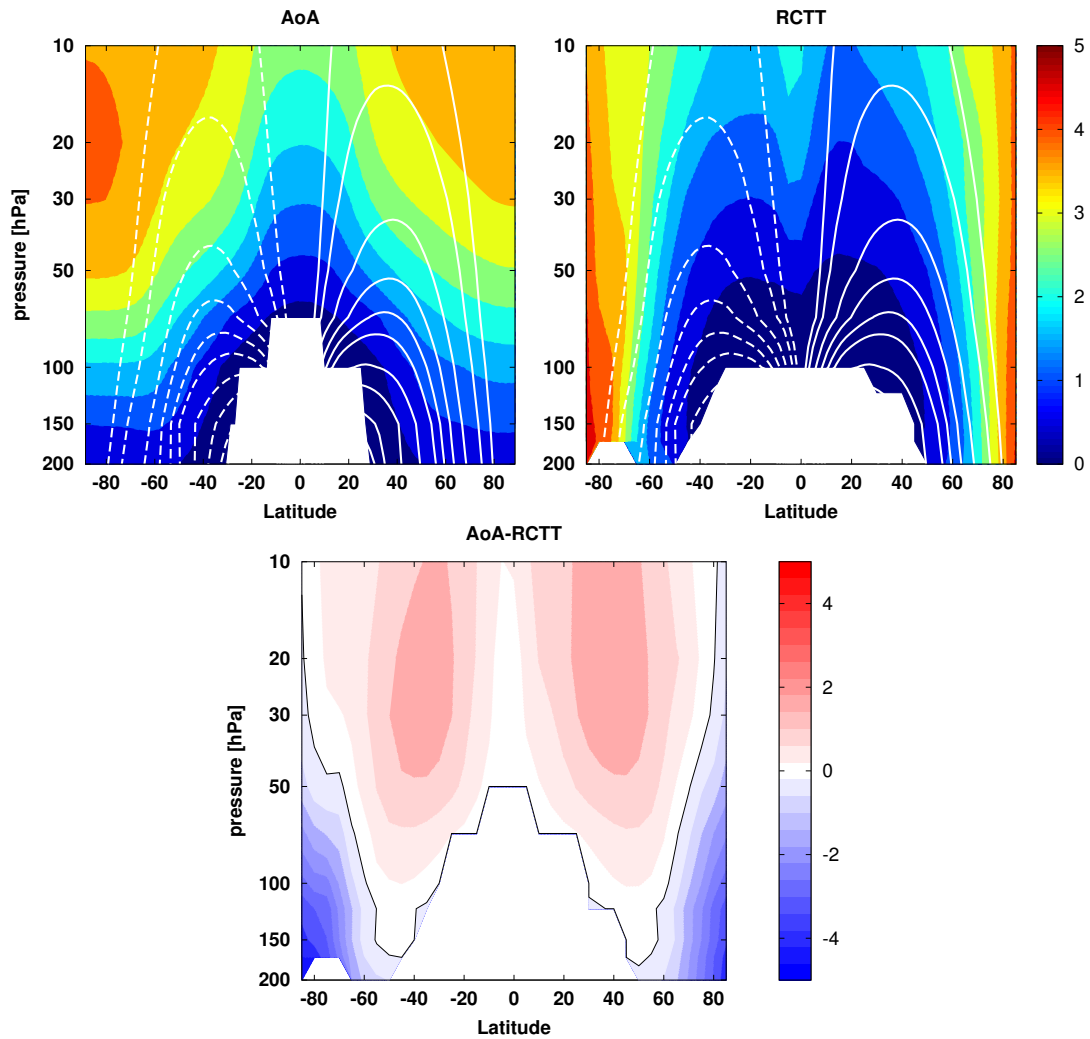
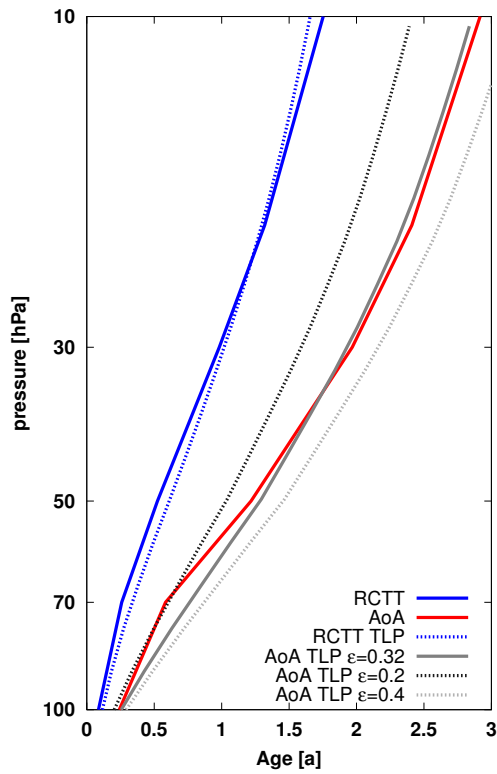


Figure 1. Illustration of stratospheric transport processes (for details, see text).



**Figure 2.** AoA, RCTT and aging by mixing (the difference AoA-RCTT) from Ecam6, TS1990, annual mean values averaged over 10 years in units of *years*. In the top panel, the annual mean residual circulation stream function is overlaid (white contours, dashed: negative; solid: positive). The thin black line in the bottom panel is the zero line.



**Figure 3.** Tropical mean ( $30^{\circ}\text{S}$ - $30^{\circ}\text{N}$ ) profiles of RCTT (blue) and AoA (red) from the GCM (TS1990) together with the results of the TLP model for RCTT (blue dotted) and AoA with  $\epsilon = 0.2$  (dark gray dashed),  $\epsilon = 0.4$  (light gray dashed) and the best fit to the GCM data with  $\epsilon = 0.32$  (gray solid).

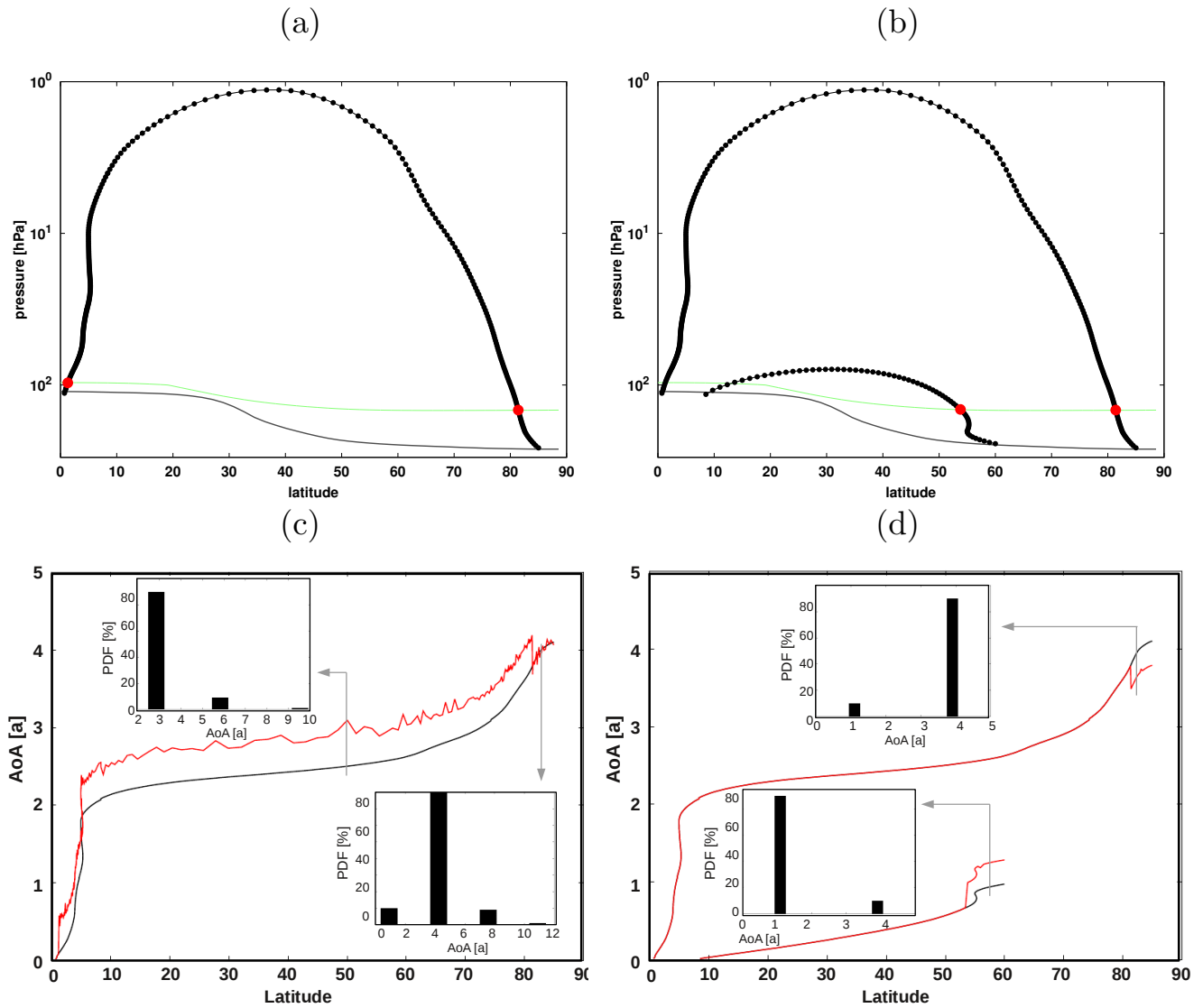


**Figure 4.** Illustration of the effects of mixing on age. Left: mixing of tropical and extratropical air from the deep circulation branch. Right: mixing of extratropical air from the shallow and the deep branch. Top panels show the example trajectories and the mixing points at 380 K (red dots, 380 K isentrope as green line, tropopause as thin black line). Bottom: mean age along the trajectory (here shown as function of latitude) without mixing (black) and after integration over 10 times the trajectory length (red). Inlets show age spectra at indicated points.

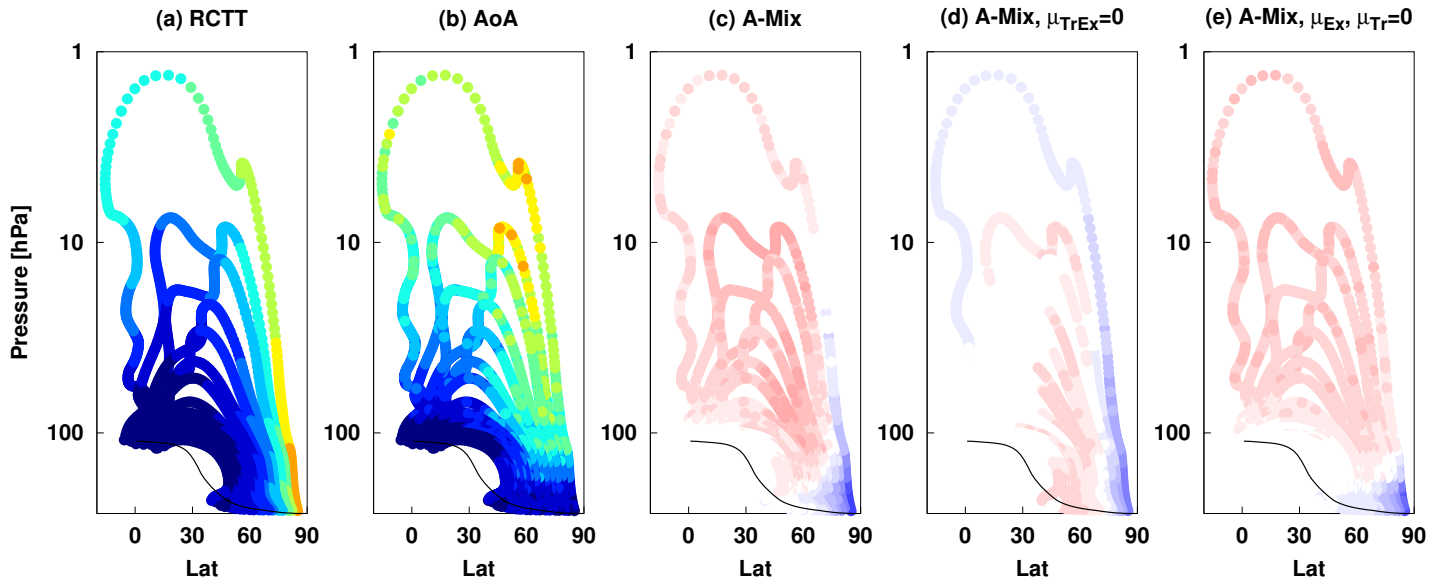


**Figure 5.** (a) RCTT, (b) AoA and (c) Aging by mixing simulated with the Lagrangian random walk model using 20 trajectories. (d) Aging by mixing for mixing only within the tropics and within the extratropics, (e) Aging by mixing for mixing only between tropics and extratropics. Color shading as in Fig. 2.

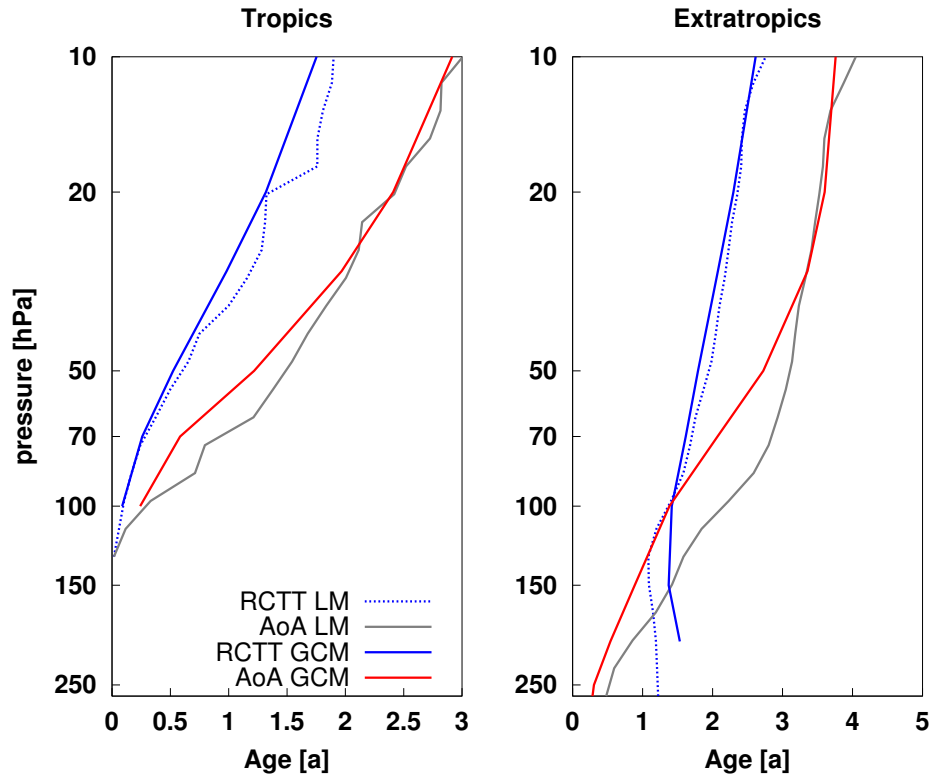


**Figure 6.** Tropical ( $0 - 30^\circ\text{N}$ ) and extratropical ( $35 - 90^\circ\text{N}$ ) mean profiles of RCTT and AoA from the GCM (blue and red solid) and the Lagrangian random walk model using 20 trajectories (blue dashed and gray).

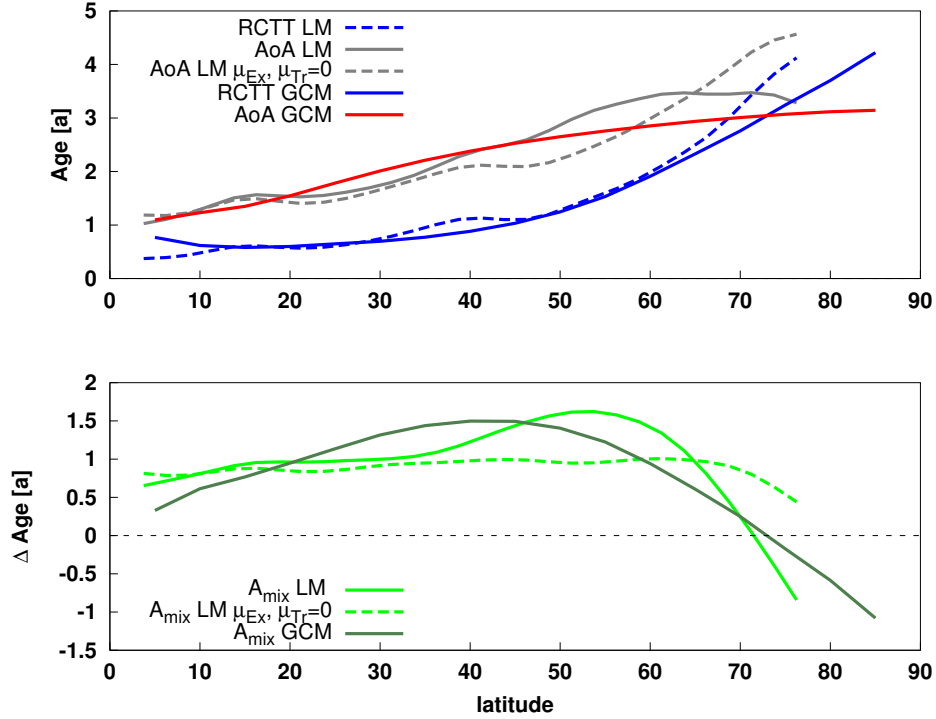


**Figure 7.** Mean latitudinal distribution averaged over 70-10 hPa of RCTT (solid blue) and AoA (solid red) from the GCM and the Lagrangian random walk model using 20 trajectories (RCTT: blue dashed, AoA: gray). Aging by mixing ( $A_{mix} = AoA - RCTT$ ) is shown in the bottom panel from the GCM (dark green) and the Lagrangian model (light green). In addition, AoA and aging by mixing from the Lagrangian random walk model with no mixing within the tropics and within the extratropics is shown (AoA: top, gray dashed, aging by mixing: bottom, green dashed).

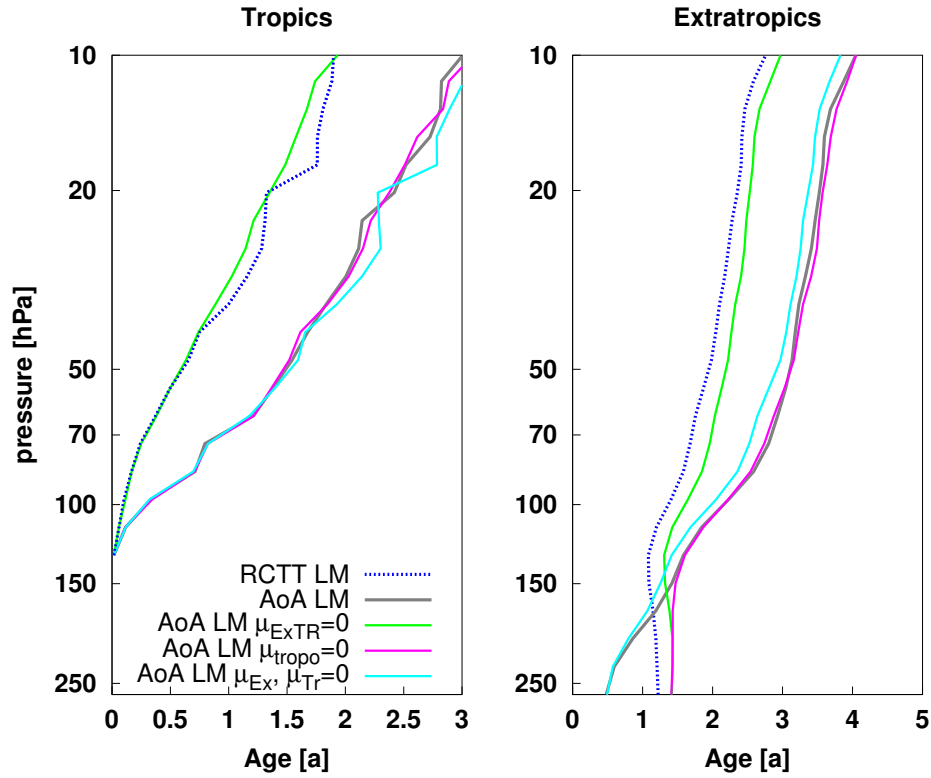


**Figure 8.** RCTT and AoA from the Lagrangian random walk model as in Fig. 6 together with profiles for sensitivity runs with the Lagrangian model without mixing between tropics and extratropics in the entire domain ( $\mu_{ExTR} = 0$ , green), without mixing in the lowermost stratosphere (i.e. no mixing below the tropical tropopause,  $\mu_{tropo} = 0$ ; magenta), and without mixing within the tropics and extratropics ( $\mu_{Ex} = 0$ , light blue).

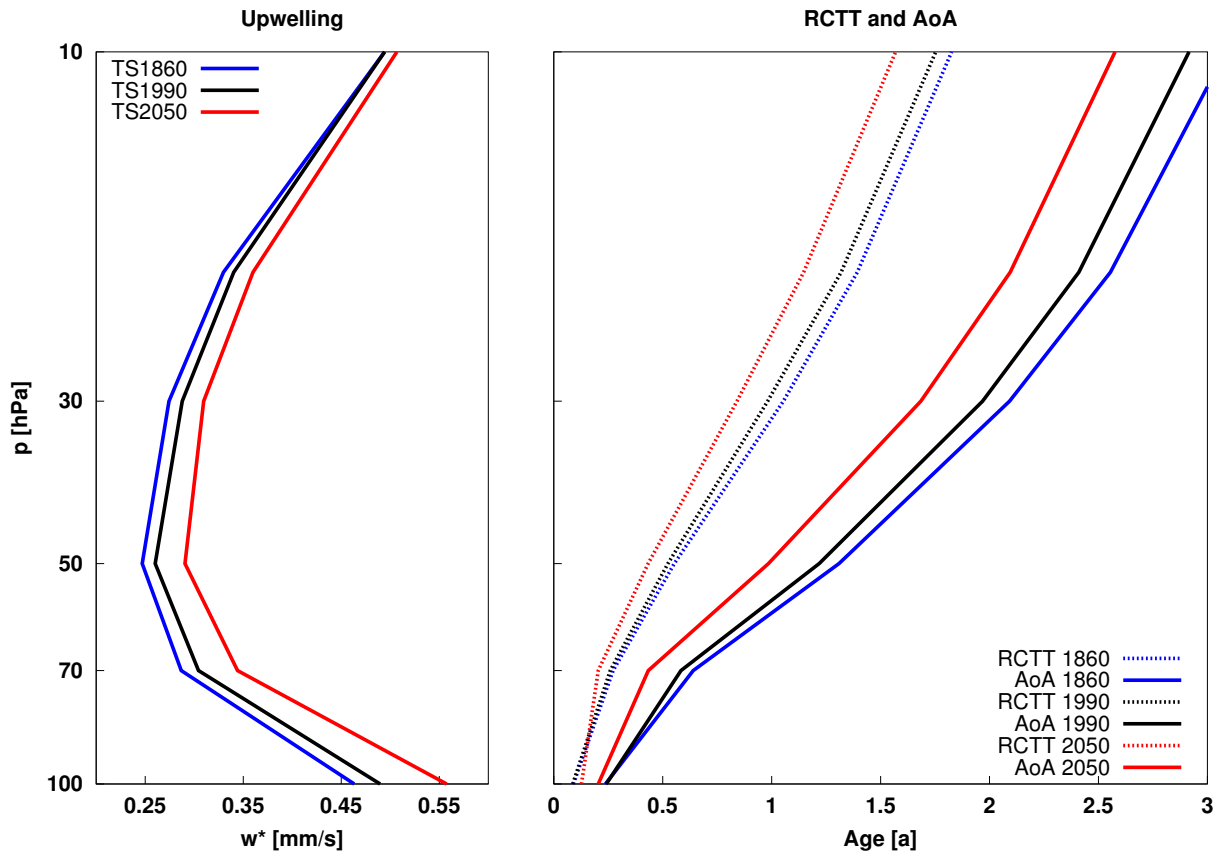


**Figure 9.** Left: Tropical mean ( $30^{\circ}\text{S}$ - $30^{\circ}\text{N}$ ) vertical residual velocity from the simulations representing 1860 (blue), 1990 (black) and 2050 (red). Right: Tropical mean ( $30^{\circ}\text{S}$ - $30^{\circ}\text{N}$ ) RCTT (dotted) and AoA (solid) from the GCM for the three simulations.

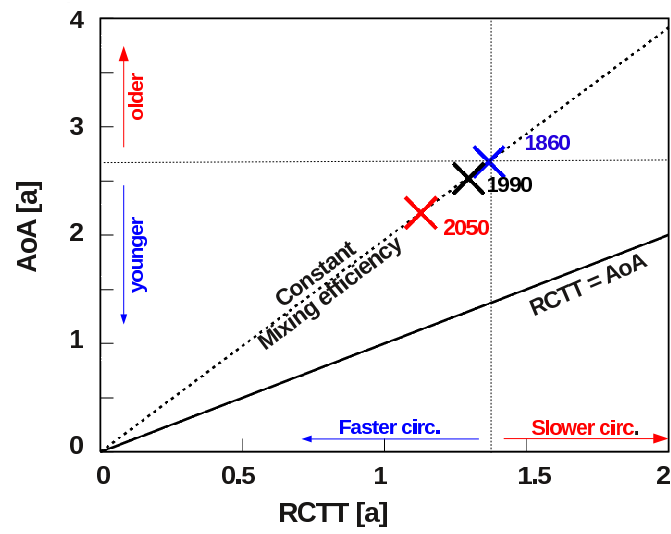


**Figure 10.** Tropical mean AoA plotted against tropical mean RCTT at 20 hPa from the 1860 (blue), 1990 (black) and 2050 (red) simulation.

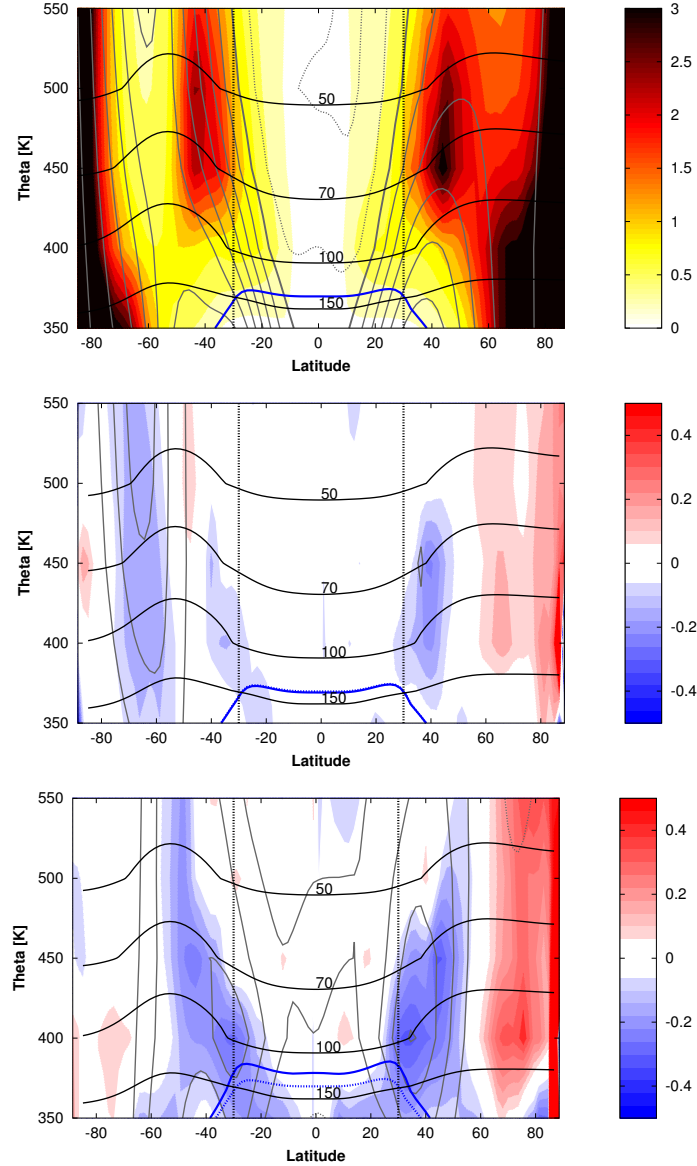


**Figure 11.** Ratio of mean PV to meridional PV gradient scaled by the earth radius ( $1/r_e PV/\frac{\partial PV}{\partial y}$ ) for the annual decadal mean from TS1990 (top) together with mean positions of pressure levels (thick black lines), zonal mean zonal wind (gray; contour interval 5 m/s, solid: positive, dotted: negative, thick line: zero) and the tropopause (blue). Relative differences in  $PV/\frac{\partial PV}{\partial y}$  for TS1990-TS1860 (middle) and TS2050-TS1990 (bottom) together with differences in zonal mean winds (contour interval 1m/s, solid: positive, dotted: negative), and the tropopause in TS1990 (dashed blue) and TS1860/TS2050 (solid blue).

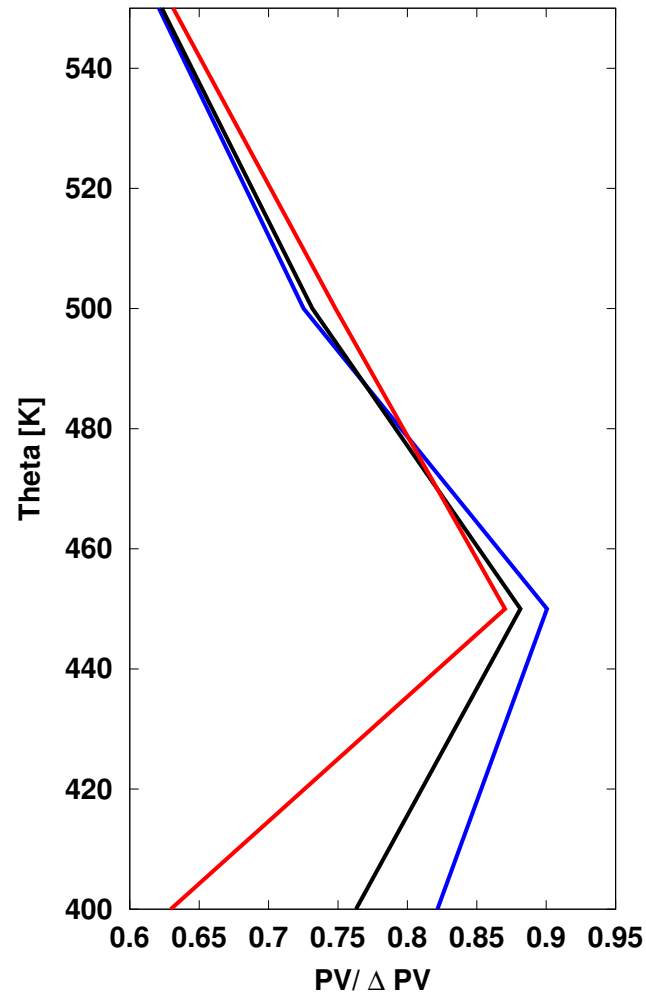


**Figure 12.** Ratio of tropical mean PV to the gradient extratropical - tropical PV for TS1860 (blue), TS1990 (black) and TS2050 (red).

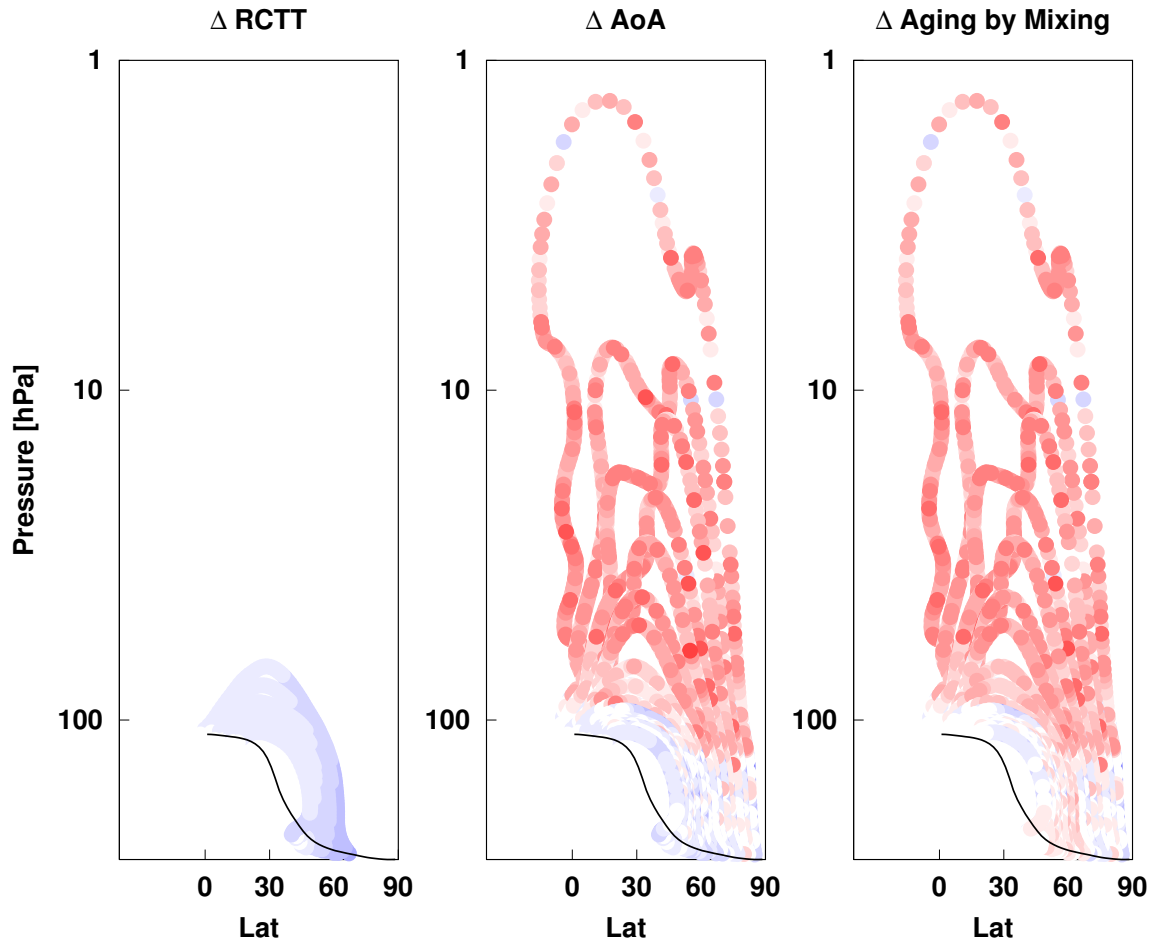


**Figure 13.** Idealized experiment with the Lagrangian random walk model resembling an intensification of the shallow branch only. Advection along the shallow branch trajectories is sped up (as seen in the difference to the base case in RCTT, left) and the mixing fraction is enhanced in the lower part so that the mixing efficiency remains constant. The resulting change in AoA and aging by mixing compared to the base case is shown in the middle and right panels. Color shading as in Fig. 2.

|              | No Mixing | Base | $\mu_{TrEx} = 0$ | $\mu_{Ex}, \mu_{Tr} = 0$ | $\mu_{tropo} = 0$ | $\mu_{TrEx}^{\Theta > 500K} = 0$ | $\mu_{TrEx}^{\Theta < 500K} = 0$ |
|--------------|-----------|------|------------------|--------------------------|-------------------|----------------------------------|----------------------------------|
| GM AoA       | 1.25      | 1.69 | 1.30             | 1.66                     | 1.84              | 1.61                             | 1.32                             |
| GM $A_{Mix}$ | 0.0       | 0.44 | 0.05             | 0.41                     | 0.59              | 0.36                             | 0.07                             |

**Table 1.** Global mean AoA and aging by mixing (in years) for different cases calculated with the Lagrangian random walk model: integration without mixing (“No mixing”), full integration with base parameter settings (“Base”), without mixing between tropics and extratropics ( $\mu_{TrEx} = 0$ ) and without mixing within the extratropics and tropics ( $\mu_{Ex}, \mu_{Tr} = 0$ ). The case  $\mu_{tropo} = 0$  refers to setting mixing between the tropics and extratropics below the tropical tropopause to zero (i.e. no in-mixing of tropospheric air), and in the cases  $\mu_{TrEx}^{\Theta > 500K} = 0$  and  $\mu_{TrEx}^{\Theta < 500K} = 0$  tropical-extratropical mixing above and below 500 K is set to zero, respectively.

|              | Base | $\epsilon$ |      | $\Theta$ level | Ntraj |      |
|--------------|------|------------|------|----------------|-------|------|
|              |      | 0.4        | 0.2  | 37             | 10    | 40   |
| GM RCTT      | 1.25 | 1.25       | 1.25 | 1.25           | 1.39  | 1.21 |
| GM AoA       | 1.69 | 1.91       | 1.50 | 1.68           | 1.95  | 1.58 |
| GM $A_{Mix}$ | 0.44 | 0.66       | 0.25 | 0.43           | 0.56  | 0.37 |

**Table 2.** Global mean (GM) AoA, RCTTs and aging by mixing (in years) as simulated in the Lagrangian random walk model for the base case, and sensitivities to the mixing efficiency  $\epsilon$ , the number of isentropic mixing levels, and the number of trajectories used.